ACS APPLIED MATERIALS & INTERFACES

www.acsami.org

Research Article

Charge-Reduced Particles via Self-Propelled Electrohydrodynamic Atomization for Drug Delivery Applications

Trung-Hieu Vu,* Sharda Yadav, Canh-Dung Tran, Hong-Quan Nguyen, Tuan-Hung Nguyen, Thanh Nguyen, Tuan-Khoa Nguyen, Jarred W. Fastier-Wooller, Toan Dinh, Hoang-Phuong Phan, Hang Thu Ta, Nam-Trung Nguyen, Dzung Viet Dao, and Van Thanh Dau*

Cite This: *ACS Appl. Mater. Interfaces* 2023, 15, 29777−29788

Read Online

ACCESS | Metrics & More | Article Recommendations | Supporting Information

ABSTRACT: Electrohydrodynamic atomization (EHDA) provides unparalleled control over the size and production rate of particles from solution. However, conventional methods produce highly charged particles that are not appropriate for inhalation drug delivery. We present a self-propelled EHDA system to address this challenge, a promising one-step platform for generating and delivering charge-reduced particles. Our approach uses a sharp electrode to produce ion wind, which reduces the cumulative charge in the particles and transports them to a target in front of the nozzle. We effectively controlled the morphologies of polymer products created from poly(vinylidene fluoride) (PVDF) at various concentrations. Our technique has also been proven safe for bioapplications, as evidenced by the delivery of PVDF particles onto breast cancer cells. The combination of simultaneous particle production and charge reduction, along with its direct delivery capability, makes the self-propelled EHDA a versatile technique for drug delivery applications.

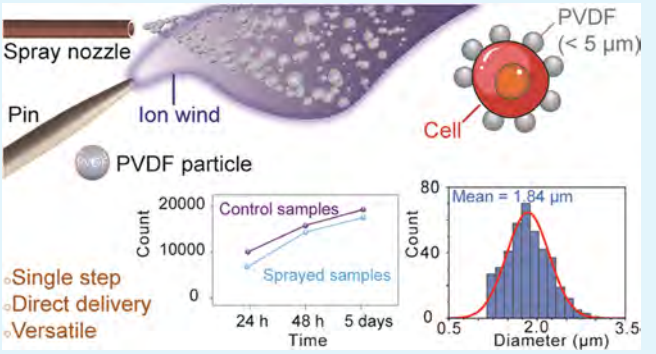

KEYWORDS: *electrohydrodynamic atomization, charge-reduced particles, single-step EHDA, ion wind, single-step drug delivery, electrospray*

INTRODUCTION

Therapeutics by particulate inhalation, via the oral or nasal route, represent a noninvasive and self-administrative approach for drug delivery in local respiratory systems or throughout the systemic body of a human being.[1,2] Pulmonary drug delivery possesses prominent advantages over conventional therapeutics such as oral or parenteral drug deliveries in terms of digestion degradation. Studies show that monodisperses of 1−5 μm bronchodilator particles are optimal in terms of drug delivery efficacy inside the human body.[3] However, other experiments also note that the range of optimal aerosol particle sizes may be much smaller than 1−5 μm, covering a range of 2.0−3.5 μm.[4,5] Some existing technologies that allow atomization of particles within this range size include jet nebulizer, vibrating mesh nebulizer, pressurized metered dose inhaler, or dry powder inhaler.[6,7] In the past decade, surface acoustic waves (SAWs), which utilizes vibration, have been emerging as a new approach to nebulize solution into monodisperse particles for medical applications.[8−11] Another method with high potential in the field of nebulization is electrospraying (ES), which combines electricity and dispersal of fluid.

Electrospraying, also known as electrohydrodynamic atomization (EHDA), is a simple but versatile technique to efficiently generate micro-/nanosized particles. ES has emerged as a potential tool for drug delivery with two functions in nanomedicine: the generation and delivery of particles as carriers in respiratory treatment.[6,12−15] ES occurs at the liquid surface of a capillary's outlet when liquid flows through the capillary under an electric field.[16] A conventional ES system consists of a capillary nozzle, a grounded conductive collector, and a voltage supply connecting the two aforesaid components. When a high voltage is applied, the electric field induces a radial electrostatic pressure on the liquid surface at the nozzle outlet, which balances the capillary pressure. This pressure equilibrium creates a cone-like-shaped droplet at the nozzle tip known as a Taylor cone. When the electrical field increases, the Taylor cone gradually elongates into a liquid filament until the equilibrium between the radial electrostatic pressure and liquid surface tension is destroyed. The filament is subsequently ejected into a mist of droplets. The droplets are ionically

Received: February 12, 2023
Accepted: May 15, 2023
Published: June 15, 2023

https://doi.org/10.1021/acsami.3c02000
ACS Appl. Mater. Interfaces 2023, 15, 29777−29788

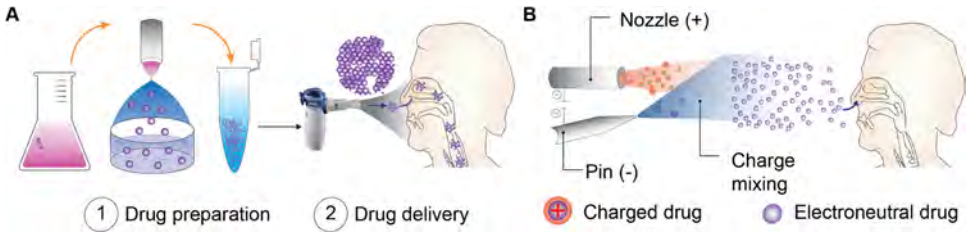

Figure 1. Concept of drug delivery via EHDA methods. (A) Electrospray enables the rapid generation of drug particles but requires additional steps to deliver particles to the desired target. This has become a challenge that limits the use of electrospray in direct drug delivery. (B) A single-step system in which particle generation is based on EHDA but it is directly delivered to the target. For this approach, the system allows three processes to occur at once: generation of particles, reduction of charge in particles, and delivery of particles to target.

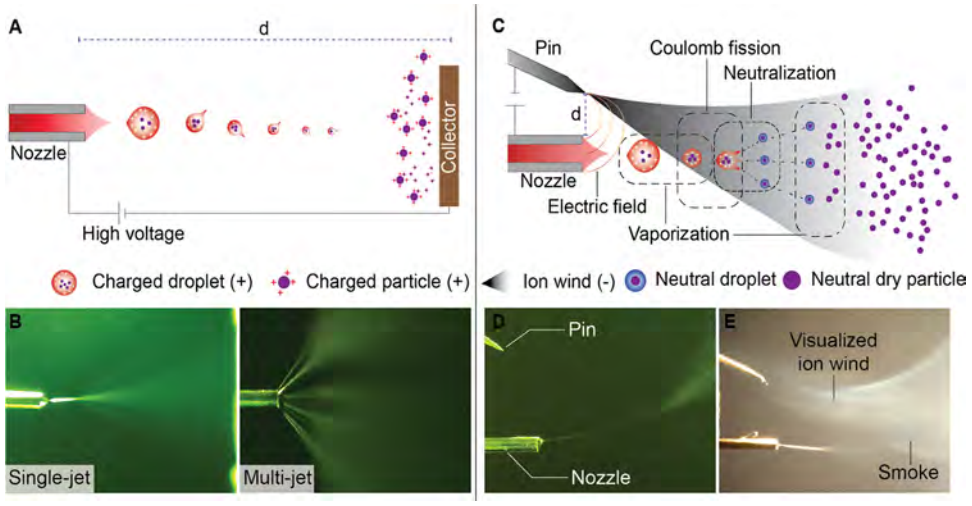

Figure 2. Conventional ES setup in comparison to our self-propelled electrohydrodynamic atomization (EHDA). (A) Schematic of the conventional ES setup in which droplets and particles are highly charged during fabrication. (B) The spray can be altered from single-jet to multijet by adjusting the supplied voltage. (C) Schematic of our self-propelled EHDA. Similar to a conventional ES system, the generated droplets using this method experience vaporization and Coulomb fission, with the additional step of neutralization. Ion wind not only propels but also neutralizes the generated particles or droplets. (D) The experimental setup consists of a nozzle and a pin placed 5 mm from each other (d = 5 mm). (E) The presence of ion wind is visualized by introducing smoke during the spraying process. As the pin generates an ion wind, it blows the smoke away from the electrode. All experiments were conducted with ethanol as the working liquid.

charged and eventually explode into smaller droplets as they reach the Rayleigh limit, the maximum value of charge a droplet can hold, and the solvent evaporates.[17] In the process, the working liquid continuously flows through the nozzle's opening and sprays a mist of droplets under the effect of the electrostatic force. The grounded conductive collector is installed in front of the nozzle and connected to the other polarity of the voltage supply, attracting the mist of droplets ejected. If the working liquid is a polymeric solution, the evaporation of solvent during the spraying process leaves dry polymeric particles at the collector.

Electrospraying is a suitable method to fabricate suitable drug particles because of its scalability and versatility.[18] After preparation of particles, they can be delivered to the desired target via inhalation using a nebulizer, dry powder inhaler, soft-mist inhalers, etc., as seen in Figure 1A.[6] The asynchronism between the collection and delivery of particles limits the ES use in applications such as drug delivery due to the additional preparation steps including but not limited to filtering, freeze-drying, washing, etc.[19−21] ES is a great technique for producing suitable particles for biomedical application; however, current applications focus on generated particles rather than the fabrication process. Figure 1B presents a concept for single-step drug delivery EHDA approach that incorporates two processes: the generation of particles and delivery of these to a desired target. This approach is expected to benefit the development of drug delivery via inhalation.

Despite the versatile use in various fields of ES, an existing problem in fabricated particles is their residual charges.[22] For drug delivery by inhalation, atomized drug particles need to be discharged. A technique that has been applied in the literature is to generate ions of opposite charge to neutralize ES particles so that they can escape the effect of reference electrode and can be conveyed to the target.[23−32] Typically, an actuator is employed to generate oppositely charged molecules to neutralize the particles from conventional ES.[33,34] Another technique involves applying alternating current (AC) instead of direct current to ES.[35,36] In this AC electrospray, oppositely charged particles are alternatively generated at suitable frequencies so that they can recombine and neutralize each other[37] or by resonating the liquid meniscus at the nozzle tip at very high frequencies.[38,39] Within the field of electro-hydrodynamic, there is a need for a solution that allows simultaneous neutralization and delivery of particles.

In this paper, we developed a novel self-propelled EHDA, which can generate and deliver charge-reduced particles in a bipolar setup. We employed two electrodes with opposite polarities in the same plane, one is a nozzle and the other is a

https://doi.org/10.1021/acsami.3c02000
ACS Appl. Mater. Interfaces 2023, 15, 29777−29788

pin with a sharp tip, to generate oppositely charged particles and ions from a single power source. In this setup, both electrodes function as the emitter and also act as the reference electrode to one another. This configuration allows the ion wind generated by the pin to coexist with the electrosprayed droplets from the nozzle electrode due to the mutual electric field between them. The ion wind impinges on the plume of electrosprayed particles and quickly reduces the total net charge in the plume. Simultaneously, the ion wind also propels the plume forward without the need for an external propeller. Unlike the multiactuator design with multiple power sources, this concept provides charge balance between the two electrodes, enabling the simultaneous generation and neutralization of particles in free space. Our device provides a simple yet efficient generation and delivery of charge-reduced particles without the use of an additional actuator or power supply. Further detailed comparison with existing techniques is discussed in Section S3 of the Supporting Information. Our method has several distinct benefits in regard to the distance travel of particles, power efficiency, and system simplicity, making it a highly attractive option for drug delivery applications.

RESULTS/DISCUSSION

Principle of Self-Propelled EHDA. In our system, droplets are simultaneously generated and neutralized in air as shown in Figure 2. A mist of particles/droplets is generated via electrostatic force from the electric field between the two electrodes, which include the capillary nozzle and the pin with a low-curvature tip. Figure 2C presents the generation of droplets in our system, which uses a similar principle to that of a conventional ES system. Under sufficient electric field applied between two electrodes, liquid surface yields the well-known Taylor cone at the output nozzle. A liquid jet emerges from the apex of the cones and breaks into fine uniform droplets. These droplets are highly charged due to the induced electric field. Simultaneously, the pin generates a negative corona discharge, which turns into ion wind of ionized air molecules. The ion wind provides sufficient propulsion force to the plume of droplets, propelling them forward. During their flight, these charged droplets interact with the air molecules of opposite charge, resulting in the reduction in total net charge in them. Particles are also formed during this process because of the evaporation of solvent as droplets are continuously fabricated. The interaction between charged droplets, formation of particles, and ion wind is discussed in the following sections.

As mentioned, an ES system is capable of producing highly charged particles and droplets.[40,41] ES is initiated when a high electric field is applied, and an electrostatic force overcomes the surface tension of a liquid. As charged particles contact the grounded substrate, they are neutralized by exchanging electrons with each other. Thus, in conventional ES, the neutralization process is completely separated from the atomization process, as shown schematically in Figure 2A. Varying the voltage controls the spraying modes, with low voltage for single-jet mode and high voltage for multijet mode.[43]

The key idea of our approach is to simultaneously generate and neutralize charged droplets in air by using a point-to-pin EHDA system. In this system, point refers to the tip of the capillary nozzle where liquid is extruded to form a Taylor cone, and the spraying process is initiated. The pin refers to the second electrode, which is placed in the same plane of the capillary nozzle and at a selected distance, d, from the nozzle axis, as described in Figure 2C. A threshold voltage applied between the two electrodes causes the liquid to form a Taylor cone at the tip of the capillary nozzle. The apex of the cone then disintegrates into a plume of smaller droplets (indicated as red droplets in Figure 2A) as the voltage increases. This spraying process is similar to conventional ES as the charge in droplets exceeds the Rayleigh limit. The induced electric field also causes the pin to produce ion wind from corona discharge, which is used to neutralize the droplets.[44] During the spraying process, similar to a conventional ES system, the droplets become positively charged and undergo Coulomb fission and vaporization. However, the negatively charged molecules in the ion wind neutralize the particles upon collision. The ion wind not just neutralizes the droplets but also propels the plume and provides it with a constant forward momentum, resulting in a plume of neutral particles flying forward (Figure 2C).

Our system aims to generate, neutralize, and deliver particles to a target simultaneously. With the initial momentum from the corona discharge, an ion cloud moves away from the electrode tips in a direction parallel to the pin electrode, as visualized in Figure 2E.[44] The ion wind is visualized by introducing smoke to the vicinity of the pin electrode (see Figure S1 for the use of smoke in the experiment). The smoke displays the presence of the ion wind and how it influences the mist of droplets (Movie S1 presents this influence). The mist consists of droplets and charged and neutralized particles (as the solvent evaporates, the droplets become polymeric particles), which are carried away from the electrodes by the ion wind. Unlike the charged particles generated from the conventional ES system, the fabricated particles in our system are neutralized during the delivery process; hence, they can be delivered to any collector placed downstream. Because of the generation of an equal ratio of positively charged particles and negative ions by the electrospray and the corona discharge, our approach can generate droplets with a lower net charge. The two processes, ion wind generation by corona discharge and particle generation, of the present self-propelled EHDA system are discussed in the following sections.

The ion wind has three main functions: (i) emitting droplets sprayed from the capillary, (ii) propelling, and (iii) driving the stream of airborne particles. The characterization of ion wind depends mainly on the geometry of the pin's tip. Hence, three pins with different sphere radii (SRs) at the tip were chosen for our experiments, with ethanol as the spraying liquid to investigate the discharge current and generation of ion wind. Pins 1, 2, and 3 had a spherical radius of 30, 35, and 130 μm, respectively. The onset of the electric field to initiate corona at a spherical tip is directly influenced by the radius, according to Peek's law[45]

$$E_w = E_o(1 + 2.62 \times 10^{-2}/R_c^{1/2}) \quad (1)$$

where $E_o = 3.23 \times 10^6$ V/m,[46] and R_c is the tip SR. The values are 18.7×10^6, 17.5×10^6, and 10.7×10^6 for pins 1, 2, and 3, respectively. This onset electric field indicates the value at which corona discharge is initiated and the appearance of ion wind for each pin. The theoretical onset voltage for the spraying process of droplets to start is[47]

$$V_o = \sqrt{\frac{\gamma R_o}{\varepsilon_o}} \ln \frac{4d}{R_o} \quad (2)$$

https://doi.org/10.1021/acsami.3c02000
ACS Appl. Mater. Interfaces 2023, 15, 29777−29788

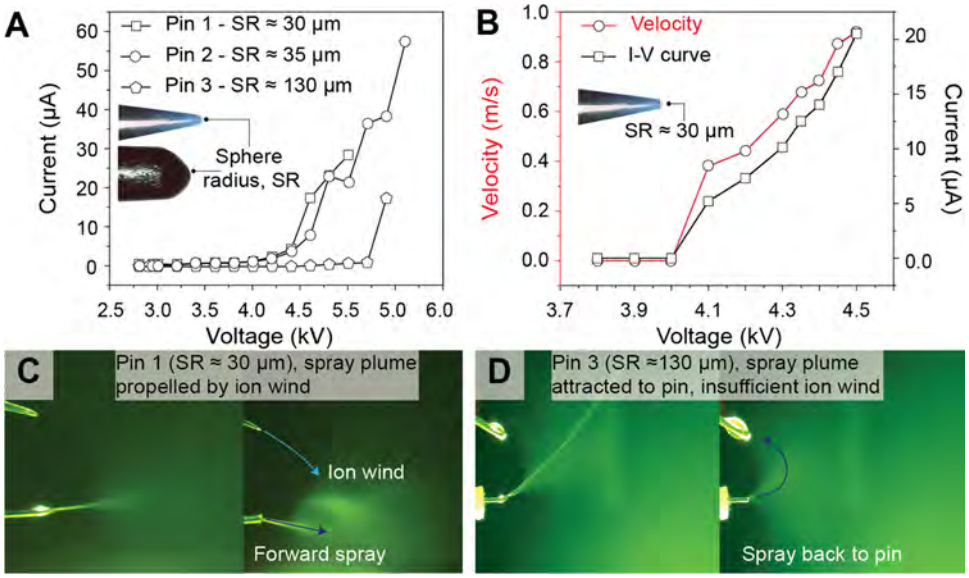

Figure 3. Characteristics and spraying behavior of the present electrohydrodynamic atomization system with pins of different tip radii. (A) Current−voltage (I−V) characteristics using different pin electrodes with three discrete tip radii. (B) The velocity, voltage, and discharge current of the ion wind of the present system using pin 1 (sphere radius [SR] ≈ 30 μm). (C, D) Spray plume is under the effect of ion wind. Sufficient ion wind blows the plume away, and insufficient wind cannot propel the plume forward, causing generated droplets to spray back to the pin.

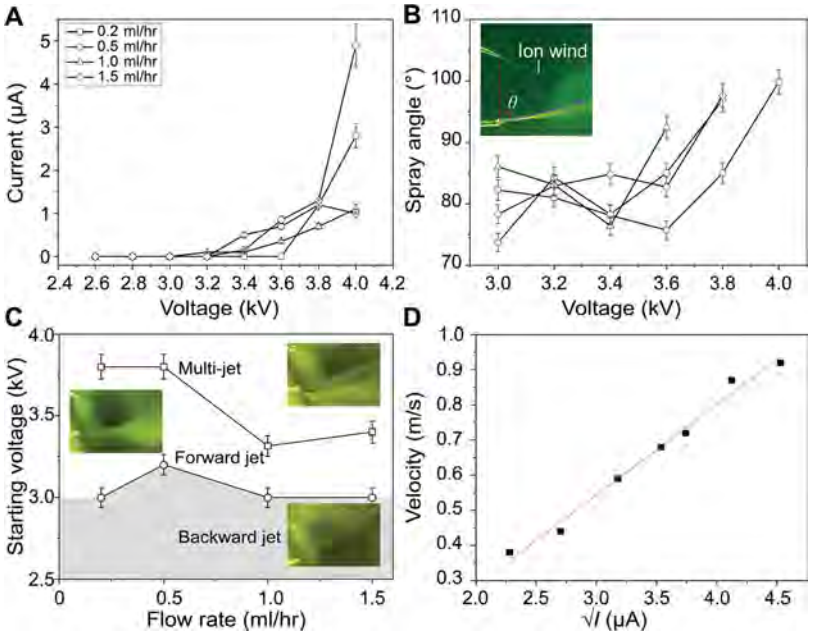

Figure 4. Characteristics of I−V relationship, spray angle, and spray modes as the flow rate increases in the self-propelled EHDA. (A) I−V characteristic for a range of flow rates: 0.2, 0.5, 1.0, and 1.5 mL/h. (B) Relationship between the applied voltage and spray angle. Higher voltage results in a stronger ion wind and a wider spraying angle θ. The pin has a sphere radius (SR) of 35 μm for optimal spray. Legends of flow rates are presented in panel (A). (C) Voltage plotted against the flow rate for the three spraying modes: backward jet, forward jet, and multijet. (D) The linearity between $\sqrt{I} - U$ describes the increasing intensity of ion wind as voltage increases.

where γ, ε_o, R_o, and d are the liquid's surface tension, vacuum dielectric constant, nozzle's outer radius, and distance between the two electrodes, respectively. The estimated value of V_o = 3 kV agrees well with our experiments for all flow rates and pin sizes. Figure 3D shows the spraying process in which a plume of droplets is attracted toward the pin and does not fly forwards due to the lack of an ion wind. This is an example in which the onset voltage is achieved for the spraying process, but ion wind is insufficient to propel the plume of droplets. The electric field of a rounded tip is derived as[48]

$$E_{tip} = -\frac{2V/R_c}{\ln\left(\frac{4d}{R_c}\right)} \quad (3)$$

where E_{tip} is the electric field at the pin's tip, and V is the applied voltage. The E_{tip} of pins 1, 2, and 3 is 30.8 × 10^6, 27.0 × 10^6, and 9.2 × 10^6 V/m, respectively, for the onset voltage V = 3 kV. Subsequently, pins 1 and 2 can generate corona discharge and ion wind because $E_{tip} > E_w$ at V = 3 kV, while pin 3 needs a voltage of $V \geq 3.5$ kV because of its greater SR. In

https://doi.org/10.1021/acsami.3c02000
ACS Appl. Mater. Interfaces 2023, 15, 29777−29788

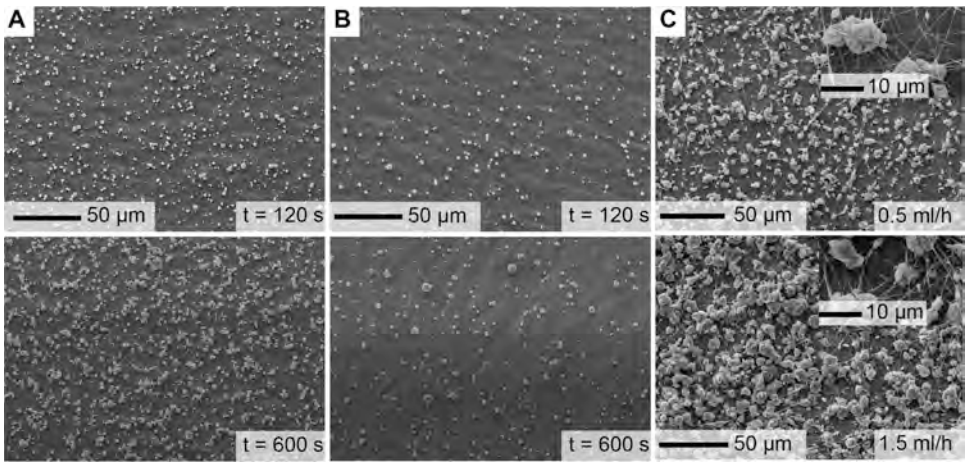

Figure 5. Fabricated products from experiments using our self-propelled electrohydrodynamic atomization system. (A, B) Fabricated poly(vinylidene fluoride) (PVDF) particles from PVDF 5 wt % at two collecting distances, 5 and 8 cm, for 120 and 600 s, respectively. Solution is sprayed at a flow rate of 0.3 mL/h, 3.7−4.5 kV voltage, and with pin 2 (sphere radius [SR] ≈ 35 μm). (C) The fabricated products as flow rate increases. The collecting distance and voltage were kept constant at 5 cm and 3.7−4.5 kV, respectively. The thin fiber strands and deformed particles suggest incomplete solvent evaporation during the spray. Scale bar in the figure is 50 μm.

other words, pins with low curvatures (pins 1 and 2) can efficiently generate ion wind as soon as the onset voltage is achieved. The graph in Figure 3A shows how pins with a greater SR require a higher voltage to initiate corona, indicated by the sudden jump in current as voltage increases. A greater current is equivalent to greater corona discharge and ion wind (Figure 3B) for the experiment with a sharp pin (SR ≈ 30 μm). However, pins with low curvature are prone to in-air shorting at elevated voltage (Figure S2). As seen in Figure 3C,D, a pin with a low curvature can simultaneously disintegrate and propel the droplets, whereas a pin with a greater SR can only disintegrate droplets and is unable to generate sufficient propulsion. A pin with greater curvature fails to generate sufficient ion wind. In such cases, jets of droplets tend to appear and wet the pin electrode, as seen in Figure 3D, which destabilizes the spraying process and causes droplets to be further attracted to the pin.

We used isopropyl alcohol as the working solution and pin 2 (SR ≈ 35 μm) to investigate the spraying behavior of our approach. The response of the system to increasing voltage between the capillary electrode and pin electrode was thoroughly studied. The range of flow rates was 0.2−1.5 mL/h, estimated from $Q = (\gamma\varepsilon\varepsilon_0)/\rho K = 1.59$ mL/h for a stable Taylor cone, where Q, γ, ε, ε_0, ρ, and K are the flow rate, surface tension, relative permittivity, vacuum dielectric constant, liquid's density, and conductivity, respectively. Figure 4A shows the $I-V$ characteristics of the system. In the previous literature, the relationship $I/V \propto V$ (Townsend relationship) was used in the analysis of corona discharge.[46,49,50] However, we found that the $I-V$ relationship in our self-propelled EHDA best-matched with the linear relationship $\sqrt{I} \propto V$, which appears less frequently in the literature.[51] In contrast, the linear relationship between velocity and current is $\sqrt{I} \propto U$, according to the equation defined by Robinson as $U = k\sqrt{I/\rho\mu}$,[46] where U is the velocity of the ion wind, k depends on the electrode discharge area and the distance between two electrodes (Figure 4D), μ is the ion mobility, and ρ is the air density.[46] This relationship is presented in Figure 4D, with the maximum velocity value of 0.9 m/s. Details of the experimental setup for velocity measurement are included in Figure S1. The linearity between current and velocity, $\sqrt{I} - U$, defines the wind intensity according to the increase in applied voltage.

We investigated the relationship between voltage and the spraying angle θ, an angle created between the spraying jet and an imaginary vertical axis, as seen in Figure 4B (inset), to display the controllability of the spraying process of this method. With increasing strength of the ion wind, the angle θ increases and approaches closer to 90°, which is equivalent to a stable horizontal spray jet. The observable spraying modes are (i) backward jet mode, when a plume of droplets can be seen flying toward the pin electrode, creating $\theta < 90°$; (ii) forward jet mode, when a straight jet with $\theta \approx 90°$ and no droplet flies toward the pin; and (iii) multijet mode, when multiple spraying jets are observed and θ cannot be defined. As mentioned earlier, the modes are correlated to the generation of ion wind, with an insufficient ion wind corresponding to the backward jet mode (as seen in Figure 2D), a sufficient ion wind corresponding to the forward jet mode and high voltage resulting in a strong ion wind and multiple spraying jets. During the spraying process, the droplets are attracted to the pin electrode while being neutralized and propelled by the ion wind.[52] The spraying modes can be seen in Figure 4C, with the insets representing the experimental images. Figure 4B depicts how voltage corresponds to the change in the spraying angle θ. Generally, all flow rates experienced a backward jet mode at a relatively low voltage and only gained a stable spraying plume of droplets as voltage reached 3.5 kV (Taylor cone−jet mode), which also corresponded to a strong ion wind. The forward movement of droplets indicated the existence of intense ion wind, capable of reducing the net charge in the mist. Experimental results showed that, for the present system, the steady forward jet mode was achieved and maintained for a great range of voltages, shown in Figure 4C. This mode is suitable for stable spraying and collection of fabricated products with great controllability. For instance, a steady forward jet mode was observed across the flow rate range of 0.2−1.5 mL/h for voltages from 3.0 to 3.8 kV (Figure 4C). The size distribution of particles is also influenced by the spraying mode, with the multijet mode producing a greater number of particles with larger sizes compared to the single-jet mode (see Section S2, Supporting Information). At an elevated

https://doi.org/10.1021/acsami.3c02000
ACS Appl. Mater. Interfaces 2023, 15, 29777−29788

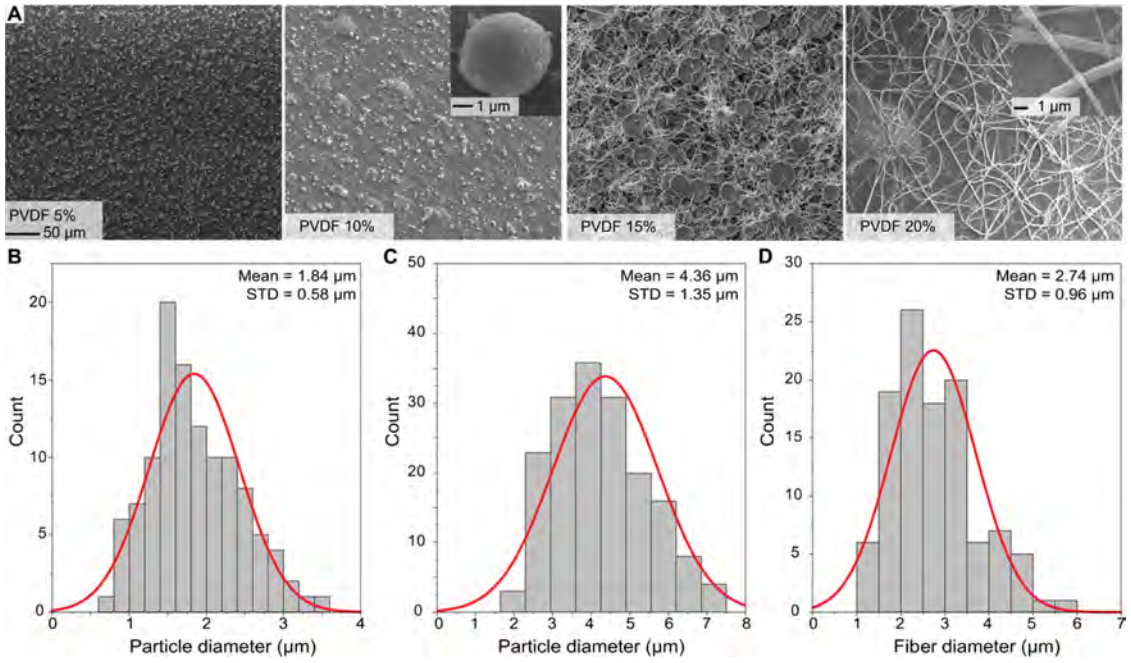

Figure 6. Controllability of fabricated products by adjusting the concentration of PVDF in solution. (A) The morphologies of particles/fibers produced from our self-propelled EHDA with different polymer concentrations. As the polymer concentration increases, fiber formation occurs. The voltage and flow rate are adjusted accordingly during the process to produce a stable spray. (B, C) Size distribution of particles generated with PVDF 5 and 10 wt %, respectively. (D) Size distribution of fibers of PVDF 20 wt %. Scale bar is 50 μm for all images.

voltage, the corona discharge comes from two sources, the pin tip and the outer of the nozzle, leading to turbulence in spray (see Figure S2 for the presence of corona discharge in the pin and nozzle). However, the ion wind's momentum from the pin is the dominant factor in the plume's movement.

Production of Polymeric Particles and Fibers. We demonstrated how our approach can fabricate and deliver not only particles but also fibers in one step. In this section, we examined solutions having various polymer contents at different flow rates and distances. The resulting particles and fibers were analyzed to determine how well the system can fabricate and deliver the final products.

Figures 5 and 6 present the fabricated polymeric particles and fibers via our point-to-pin EHDA system. Based on the preliminary results, pin 2 (SR $\approx$ 35 μm) was selected, as it is the most suitable for controlling spraying parameters. The effect of collecting distance was experimented at 5 and 8 cm. Figure 5A,B show that the particle coverage declines drastically as the collecting distance increases. Even though longer collecting distance results ensure complete evaporation of solvent, it usually causes loss in particle number. Our configuration showed successful fabrication and delivery of particles at a collecting distance of 8 cm, which is 16 times greater than the electrode distance (i.e., the distance between the nozzle and the pin, which is 5 mm). Delivery effectiveness is determined by the particle population density over a unit of area over time. This analysis is dictated by dividing the total number of particles by the area of observation. At 5 cm, the particle density is estimated to be 0.68 and 1.1 particles/μm^2 over 120 and 600 s, respectively. In contrast, this value stays almost constant, about 0.48−0.60 particle/μm^2, over both periods for 8 cm. Thus, 5 cm is more effective than 8 cm in terms of the number of particles collected. This analysis is based on scanning electron microscopy (SEM) images seen in Figure 5 and implies that there is a significant loss of particles at a long delivery distance because of external airflows from the ambient environment. Since the charge in particles is reduced, they are sensitive to external airflows and efficiency loss is expected with a long collecting distance.

The effect of flow rate was also studied and is presented in Figure 5C. The distance was kept constant at 5 cm, and the flow rate varied. Polymeric solution (poly(vinylidene fluoride) [PVDF]) of 5 wt % was supplied at 0.3 mL/h for the experiments shown in Figure 5A,B, while this value was 0.5 and 1.5 mL/h for the experiments shown in Figure 5C. The final products of the higher flow rates, 0.5 and 1.5 mL/h, displayed not only particles but also thin strands of fibers connecting the particles. The previous literature suggests that the same morphology can be observed for electrospinning PVDF 7% w/v.[42] This fiber formation is due to dependence on the electric field. There is incomplete solvent evaporation with a higher flow rate, leading to deformation and inconsistency in morphologies, as seen in Figure 5C.

Figure 6 summarizes the influence of polymer concentration on the morphology of the final polymeric products. Our point-to-pin system produced particles with PVDF solution concentrations of 5 and 10 wt %. At a higher concentration of 15 wt %, our system could produce fibers, but the morphology indicates that unevaporated solvent deformed the fiber strands. The system produced consistent fibers with a solution at a 20 wt % concentration (Figure 6A). Figure 6B−D presents the analysis of particles and fibers produced by this system. The solutions of PVDF 5 and 10 wt % produced a majority of particles smaller than 10 μm with the polydispersity indices (PDIs) of 0.099 and 0.095, respectively (Figure 6B,C). 20 wt % of PVDF could produce fibers with diameters ranging from 1 to 5 μm (Figure 6D). The quality of particles and fibers can be improved through further optimization techniques, such as adjusting the electrode distance, the choice of capillary, flow rate, or solvent ratio, etc. Among these methods, adjusting the

https://doi.org/10.1021/acsami.3c02000
ACS Appl. Mater. Interfaces 2023, 15, 29777−29788

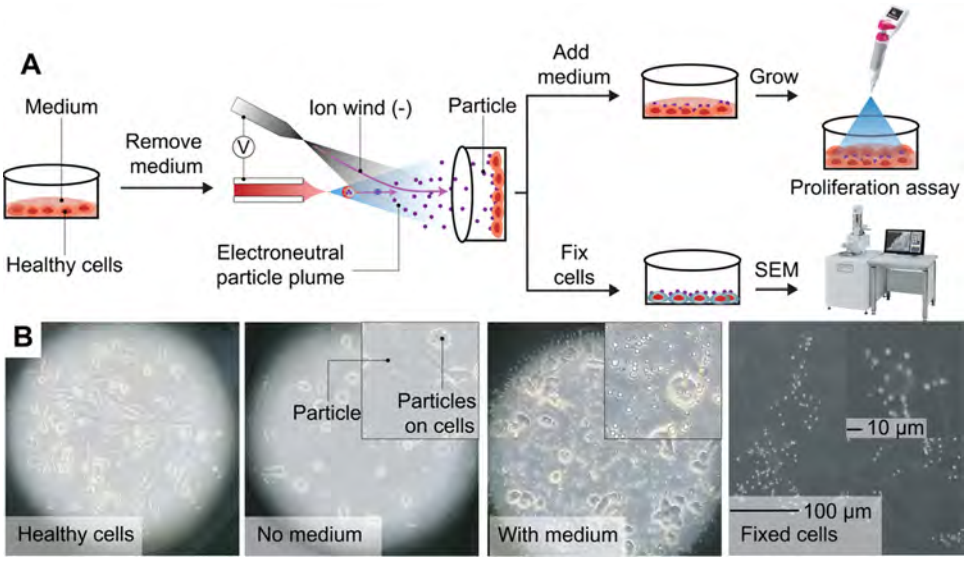

Figure 7. In vitro test of cells sprayed with PVDF particles via the present self-propelled electrohydrodynamic atomization system. (A) The step-by-step experimental procedure. Multiple cell samples are prepared for two purposes: proliferation assay and observing cells via microscope. The process involves removing and adding liquids for cell culture and cell fixation. (B) Microscopic images of cells at various stages: control sample, sprayed sample with and without medium, and scanning electron microscopy (SEM) images of fixed cells with particles adhered onto them.

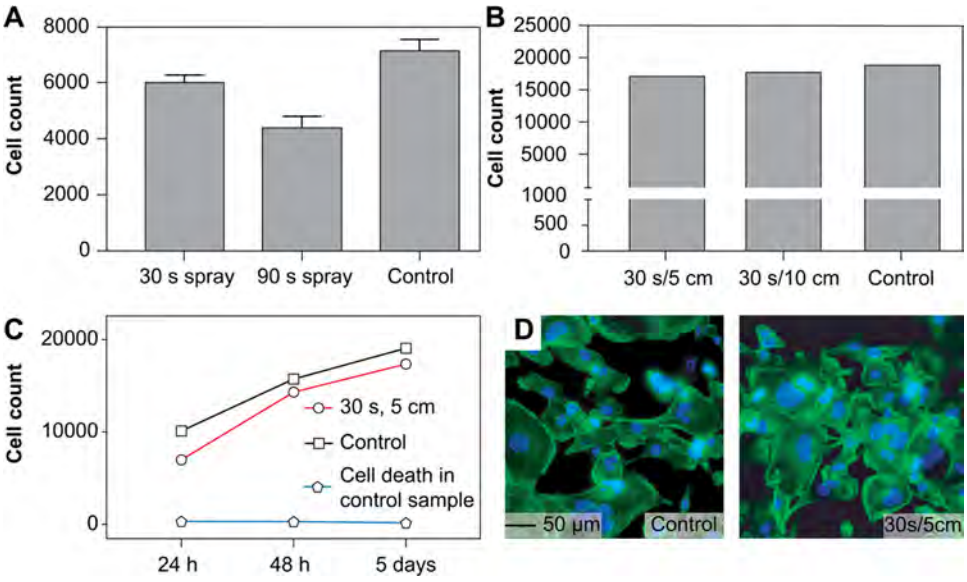

Figure 8. (A) Cell count after 2 days of two spraying periods, 30 and 90 s, at 5 cm. (B) Cell count after 5 days at two distances, 5 and 10 cm. (C) Proliferation assay of 30 s/5 cm sprayed sample over 5 days. (D) Representative fluorescence images of MDA-MB 231-cells after 2 days. Scale bar in the image is 50 μm.

solvent ratio or concentration of polymer in solution is a simple approach to enhance the quality of fibers.[43,53] The results demonstrate that our system is capable of manufacturing not only particles but also fibers by tuning the polymeric concentration. Section S2 in the Supporting Information elaborates on various morphologies of fabricated products.

Single-Step Delivery of Particles onto Cells. The ability to generate and neutralize particles makes our self-propelled EHDA system potentially suitable for pulmonary therapeutics thanks to achievable particle size, reduction in total net charge, and ease of fabrication. Therefore, our self-propelled EHDA system was tested using a breast cancer cell line (MDA-MB-231) to demonstrate the potential of safely delivering particles directly onto cells from a distance. In the test, we sprayed 5 wt % of PVDF with the present system, so the generated particles could adhere to the cells. First, we determined the morphology of the fabricated particles and how they adhere to cells by observing microscopic pictures and SEM images. Second, we analyzed how they grow over up to 5 days by comparing them with a control sample. For conventional ES approaches, the usual method of transferring particles onto cells has two steps, collection of particles and delivery to targeted cells.[54] Thus, an in vitro test could demonstrate how our self-propelled EHDA system can be a single-step solution to generate and deliver particles to cells effectively.

As shown in Figure 7A, we used our self-propelled EHDA system to simultaneously generate and deliver biocompatible PVDF particles onto Petri dishes containing cells. PVDF is

https://doi.org/10.1021/acsami.3c02000
ACS Appl. Mater. Interfaces 2023, 15, 29777−29788

biocompatible and has been used for cell culture.[55] Cells were prepared prior to the experiments (see the Methods/Experimental Section). During the spraying process, Petri dishes were placed horizontally at a distance from the nozzle tip. Cell culture medium (Dulbecco's modified Eagle's medium/nutrient mixture F12 [DMEM/F12]) had been removed prior to the spraying process, ensuring that particles could adhere to the cells and their membranes instead of mixing with the medium. In parallel, the medium of another cell group was also removed in the same amount of time to act as the control sample as seen in Figure 7A. This method ensures that both the sprayed samples and control sample would experience the same growth condition. After the particles were sprayed on the cells in the Petri dishes, the dishes were divided into two groups for further analysis—(i) with culture medium and (ii) fixed with paraformaldehyde (PFA) liquid—before being observed under a scanning electron microscope. The first group was used in the proliferation assay to investigate the growth of the particle-adhered cells, and the second group was used to observe how the particles adhered to cells immediately after the experiment. Cells were observed at multiple stages, and along with PVDF particles, viewed under a microscope (Figure 7B). Microscopic observation also showed that adding additional liquid, such as cell culture medium or PFA liquid, detached a significant number of particles from cells (Figures S9 and S10, Supporting Information). These particles float in the medium instead of adhering to cells and can be observed by changing the focal plane in the microscope (Figure S9C,D in the Supporting Information shows some particles floating in the culture medium, while some are adhered to cells). The SEM images of the cells after being fixed with PFA liquid reveal that particles were well adhered to cells (Figure 7B, far right inset). Thus, the action of putting the liquid solution into Petri dishes containing particles and cells (either medium DMEM/F12 for cell growth or PFA liquid for cell fixation) affected the adhesion between cells and particles but did not remove the particles from the cells completely.

We studied the optimal spraying time of PVDF particles generated from our self-propelled EHDA system by investigating cell growth after 2 days. As mentioned earlier, the PVDF particles were generated and delivered to the Petri dishes with the cells before medium (DMEM/F12) was added for culturing. Therefore, cells could grow and develop after the spraying experiment. PVDF is known for its high biocompatibility.[56] The results, shown in Figure 8A, indicated the difference in cell numbers at two different spraying times (30 and 90 s) at a 5 cm distance compared with a control sample after 2 days. Figure 8A shows that the number of cells was 8000 for the control sample and 6100 and 4300 particle-adhered cells for the spraying period of 30 and 90 s, respectively, at 5 cm. Multivariate analysis (analysis of variance (ANOVA)) indicates that there are statistical differences between the control group and the sprayed sample of 90 s, with the sprayed sample showing a significant reduction in cell. The similarity between the control group and the sprayed sample of 30 s implies no difference in their growth after 2 days. The main reason for cell loss is suspected to be incomplete evaporation of the solvent during the spraying process. As the solvent used to dissolve PVDF powder (*N*,*N*-dimethylformamide [DMF] and acetone [ACE]) is harmful to cells, the unevaporated solvent can negatively influence growth activity. Therefore, the evaporation rate plays an important role in effectively delivering particles to the samples. This factor is greatly affected by the generation and distance between the nozzle and collector.

The effectiveness of the spraying distance was also studied, and the results are presented in Figure 8B. Our self-propelled EHDA system was used to spray 5 wt % of PVDF at cells for a constant period (30 s) at two distances, 5 and 10 cm. Cells were counted and compared with the control samples after 5 days. A longer distance of 10 cm could improve evaporation and reduce the risk of loss of cells due to solvent (see Figures S7 and S10 in the Supporting Information). Figure 8B shows that the number of cells counted after 5 days was almost the same across the three samples. Therefore, a 10 cm distance was possible to deliver the particles to cells without causing negative influence on them by the unevaporated solvent. This distance is suitable for drug deposition in oral or nasal drug delivery since the distance for drug nebulization intake is approximately 10−20 cm.[57,58] The evaporation of solvent was also accelerated by the ion wind as seen in drying applications.[59] The results show that our system can deliver particles to cells safely at a long distance by increasing the evaporation rate of solvent.

To analyze the growth conditions of the cultured cells further, the cell activity of a sample of cells exposed to a 30 s spraying period and a collecting distance of 5 cm was assayed and compared with the control sample. The results are presented in Figure 8C. After 5 days, the growth activity of particle-adhered cell samples is similar to that of the control sample. The consistency in growth between the two samples confirmed that (i) the spraying process did not affect the growth of cells over the long proliferation period, i.e., cumulated solvent during the 30 s spray did not reduce cell number dramatically, and (ii) the successfully delivered particles did not interfere with cell growth. In addition, the fluorescence images of the control and sprayed samples after 2 days (Figure 8D) indicate almost no difference between them. They both show the usual cell attachment and spreading, with general morphology. Therefore, our self-propelled EHDA system can safely deliver particles onto cells without the risk of harming them.

CONCLUSIONS

Here, we have presented a self-propelled EHDA system as a platform for the generation of particles for drug delivery in a one-step process. This platform (i) allows for the simultaneous generation of oppositely charged particles from the pin and nozzle, (ii) can generate particles and fibers from polymeric solution, and (iii) neutralizes particles/fibers and delivers them to a target positioned downstream. The self-propelled EHDA system omits the need for an external flow, as it can deliver particles as they are generated. This approach has great potential as an effective single-step method for delivering discharged particles in drug delivery applications. In pulmonary applications, it is essential for particles to have an appropriate size and neutrality. Our system has demonstrated the ability to produce electroneutral particles within the size range of 1−5 μm, which is much smaller than the droplets produced by conventional nebulizers. Further discussion on the size range can be found in Section S3 of the Supporting Information. Additional data shown in Figure S3 demonstrates the system's ability to generate and collect particles onto floating substrates that are electroneutral and not influenced by an electric field.

https://doi.org/10.1021/acsami.3c02000
ACS Appl. Mater. Interfaces 2023, 15, 29777−29788

Our system can control the fabricated products via control of the polymeric concentration of the solution. Similar to conventional electrohydrodynamic techniques such as ES and electrospinning, the ability to generate fibers and particles has tremendous potential in various applications.[6,60] By tuning parameters such as the pin radius, flow rate, collection distance, and solution concentration, we have demonstrated how our system can be effectively controlled and refined. The performance of the EHDA system is influenced by various parameters, such as voltage, collecting distance, concentration of polymer in solution, and flow rate, as per conventional electrohydrodynamic techniques. Through experimentation, we have established that the charge-reduced particles produced by our system can travel over a considerable distance, up to 10 cm, which is appropriate for nasal drug delivery.

Factors such as ion wind, collecting distance, spray direction, density of delivered particles, and particle/fiber size were investigated by studying the morphologies of the fabricated products. The resulting particles were found to be well-suited for a variety of applications and displayed a high degree of consistency with the simple fabrication process.[22] While the fibers generated from a 20 wt % solution of poly(vinylidene fluoride) (PVDF) showed some degree of nonuniformity, further refinements have the potential to improve their quality. Another noteworthy advantage is that the targeted collector is not a part of the system, so it can be freely placed downstream from the nozzle. This is a tremendous benefit over conventional ES in which products can be directly collected on the reference electrode.[61,62] This allows flexibility to choose the collector as demonstrated in more detail in Figure S3. Furthermore, the ability of neutral particles to travel deeply into target segments of the body is of great significance for drug delivery applications.[11]

To investigate its use in practice, our system was applied in an in vitro test in which breast cancer cells were sprayed with PVDF particles via our self-propelled system and analyzed via microscopic observations and proliferation assay. Particles within micro-/nanoscale range have long been considered important in drug delivery applications, especially in the field of inhalation.[63] Previous works primarily focused on producing such particles before delivering them to the test subjects, with the generation and delivery processes being distinct from one another.[54,64] Our self-propelled EHDA system represents a novel approach as it allows for the simultaneous generation and delivery of particles, which we aimed to validate as a viable approach in biomedical applications. The results were obtained by observing the morphology of cells after spraying, and proliferation assay was conducted. The results indicated how our self-propelled EHDA system successfully generated and delivered particles onto the cell surface. More important, even though particles were washed away as liquids were added, SEM images confirmed that the loss was insignificant, as a great number of particles were well adhered to the cells (Figures S4 and 7). The adhesion between particles and cells with their membranes is strong, suggesting a potential application in the delivery of particles directly to a target. Our self-propelled EHDA system is discussed and compared further with other available systems such as atomizers and nebulizers in Section S3. PVDF is a biocompatible material, and the data indicates that the PVDF particles sprayed onto cells did not interfere with cell growth over a period of up to 5 days. The results also indicate whether the delivery process via our system is cytotoxic to the cells. As the solvent used to dissolve PVDF can reduce cell numbers and kill them directly, the solvent accumulated in a long spraying period is a noticeable risk. From preliminary data, we tested and found the optimal spraying time and distance to prevent this risk. The self-propelled EHDA system demonstrated the potential for safely delivering particles directly onto cells from a distance, and its ability for the simultaneous generation and delivery of particles was validated as a potential solution for future studies in biomedical applications.

METHODS/EXPERIMENTAL SECTION

System Preparation and Operation. The solution was ejected from a setup described in detail in Section S1 in the Supporting Information. Generally, the present system uses a 22 Ga capillary nozzle (Musashi Engineering, Japan), located 5 mm from the pin electrode at an angle of 30° (Figure 2B). The solution was stored in a syringe (1 mL, Terumo) and was fed at a constant rate using a syringe pump (Era NE-300, Adelab Scientific, Australia). A specially designed three-dimensional (3D)-printed part made of polylactic acid was used to hold the nozzle and pin in place. A DC source was the only power supply connecting to an amplifier to apply the voltage between electrodes. The collector was placed at a distance from the nozzle, unconnected to any power supply or electrical source. Collectors varied from conductive to nonconductive substrates and are described in more detail in Figure S8 of the Supporting Information. For the samples mentioned in the Results/Discussion section, the substrate was an aluminum foil held at a distance from the nozzle. For the proliferation assay, the collector was a Petri dish containing cells placed horizontally to the nozzle, as shown in Figure 7A. Other substrates, paper and acrylic sheet, were also used as collectors and are shown in Figure S3.

Three pins with varying tip radii were used to investigate the generation of ion wind. The pins were named pins 1, 2, and 3 and had an SR of 30, 35, and 130 μm, respectively. The test liquid was isopropyl alcohol (99.5%, Sigma-Aldrich) with the following specifications: surface tension $\gamma \approx 20.8$ mN/m, density $\rho \approx 0.785$ g/mL, viscosity $\mu \approx 1.66$ mPa s, conductivity $K \approx 6$ μS/m, and relative permittivity $\varepsilon \approx 18.6$. The selection of isopropyl alcohol as the working solution was due to its uniform surface tension in a concentrated electric field. The discharge current and ion wind velocity were measured and recorded using a digital multimeter (Digitech QM1535) and an air-velocity meter set (E+E Elektronik LOGPROBE61, E+E Elektronik Omniport 30). The velocity meter was placed 5 mm from the nozzle. Smoke was introduced during the spraying process to visualize the effect of ion wind on the plume of droplets.

The same polymeric was used across experiments to preserve consistency between results. PVDF powder ($M_w \approx 534\,000$, Sigma-Aldrich) was dissolved in a 4:1 ratio mixture of DMF > 99% (Sigma-Aldrich) and ACE ≥ 99.5% (Sigma-Aldrich). The solution was prepared by stirring vigorously at 40 °C for 4 h until the solution was transparent and homogeneous. The PVDF solutions varied in polymeric concentrations as the content of PVDF varied between 5, 10, 15, and 20 wt %. For particle and fiber production, pin 2 (SR ≈ 35 μm) was used for optimal results. During the fabrication process, the pin was constantly wiped with a cotton bud to prevent accumulated droplets/fibers from destabilizing the process.

Cell Preparation, Cell Spraying Procedure, and Analysis Process. Breast cancer cells (MDA-MB-231) were obtained from the American Type Culture Collection (ATCC). The cells were grown and maintained in DMEM/F12 culture medium (Gibco, Thermo Fisher Scientific, Waltham, MA) with a mix of 10% fetal bovine serum (FBS) and 1% penicillin/streptomycin. The cells were cultured in a T75 flask at 37 °C in a humidified atmosphere with 5% CO_2. Once they reached an 80% confluence, they were washed with Hanks' balanced salt solution (HBSS), harvested with a prewarmed dissociation reagent TrypLE, and observed under a microscope for detachment. 80% confluent cells were harvested and counted with a hemocytometer; a total number of 5000 cells were seeded into the

https://doi.org/10.1021/acsami.3c02000
ACS Appl. Mater. Interfaces 2023, 15, 29777−29788

Petri dish. When cells were detached, the medium was added and centrifuged at 200*g* for 5 min. Cells were then suspended and counted using a hemocytometer before being seeded into small Petri dishes (35×15 mm^2) and incubated at the same conditions for 24 h before experiments were undertaken to achieve optimal adherence and growth of the cells on the membrane. For each experiment presented in Figure 8, multiple samples were prepared prior to the proliferation assay experiments. For example, the optimal spraying time from 5 cm in Figure 8A,D used three Petri dishes, one control and two sprayed samples.

The experimental setup for delivering 5 wt % of PVDF particles onto cells seeded in Petri dishes is described in Figure 7A. The setup consists of a 22 Ga nozzle (Musashi Engineering) and pin 2 (SR ≈ 35 μm) placed 5 mm from the nozzle (electrode distance is 5 mm). The flow rate was kept constant at 0.5 mL/h, with the applied voltage being adjusted within the range of 4.8−5.3 kV for a stable spray. Prior to the experiments, the culture medium was removed and the dish containing the cells was placed vertically to the ground from the nozzle, as seen in Figure 7A. This maximized the solvent evaporation rate and reduced the risk of dripping solvent into the dish. Cells were observed under a microscope before and after the spraying process, with and without the medium (Figure 7B). The spraying time and distance of each experiment are indicated earlier.

Before each experiment, the DMEM/F12 medium was removed so that the generated particles could adhere to the cell surface. After spraying the PVDF particles, the Petri dishes of cells were used for two purposes: proliferation assay and surface morphology analysis. Thus, the cells were divided into two groups, one with the added medium (DMEM/F12) and the other fixed with 4% PFA to be observed under a scanning electron microscope. The first group was kept in the incubator at 37 °C for optimal growth before being counted. For the proliferation assay, cell samples were observed closely and counted as indicated in Figure 8A−C. For counting, the cells were detached and collected before dye from a cell-counting kit (WST-8, Abcam) was added. Cells were counted by colorimetric method. For the second group, we left the PFA to evaporate completely for 2 h and applied sputter gold before SEM observation. SEM images were acquired from a JSM-6510LV (JEOL). All images were sputtered with gold from a K575X sputter coater (Emitech). We performed statistical analysis of all experiments using Prism 8 software (GraphPad Software, San Diego, CA). We followed the standard process of immunofluorescence staining to observe the cells after 2 days of growth. Cells were fixed with 4% PFA for 15 min before being washed with HBSS (three times). Then, the cells were stained with ActinGreen 488 (Thermo Fisher Scientific) and NucBlue ReadyProbe reagents, followed by incubation at room temperature for 30 min. The stained cells were washed three times with HBSS solution at 4 °C until imaging and analysis. The images of cell nuclei and actin fibers were obtained with a fluorescent microscope (Nikon Eclipse Ti2).

■ ASSOCIATED CONTENT

Supporting Information

The Supporting Information is available free of charge at https://pubs.acs.org/doi/10.1021/acsami.3c02000.

Charge reduction in ES via ion wind (Section S1); controllability over the formation of polymeric particles/fibers (Section S2); self-propelled EHDA with respect to atomization and drug delivery technologies (Section S3); schematic of the experimental setup (Figure S1); charge measurement (Figure S2); visualization of charge-reduced particles (Figure S3); spraying behavior as voltage increases and destabilization in spraying due to accumulated droplet (Figure S4); size distribution of IPA in different modes (Figure S5); morphologies of various polymers at a 5 wt % concentration at a 10 cm distance (Figure S6); PVDF 5 wt % collected at 10 cm on fixed cells (Figure S7); deposition of PVDF particles onto free collector made from various materials (Figure S8); deposited PVDF particles on Petri dishes of cells under a conventional microscope and SEM (Figure S9); and deposited PVDF particles on Petri dishes of cells after spraying at various distances (Figure S10) (PDF)

Smoke visualizes ion wind during the generation and delivery of particles (Movie S1) (MP4)

■ AUTHOR INFORMATION

Corresponding Authors

Trung-Hieu Vu − *School of Engineering and Built Environment, Griffith University, Gold Coast, QLD 4215, Australia;* orcid.org/0000-0003-4431-1874; Email: trunghieu.vu@griffithuni.edu.au

Van Thanh Dau − *Centre for Catalysis and Clean Energy, Griffith University, Gold Coast, QLD 4215, Australia;* orcid.org/0000-0002-8242-9884; Email: v.dau@griffith.edu.au

Authors

Sharda Yadav − *Queensland Micro and Nanotechnology Centre, Griffith University, Brisbane, QLD 4111, Australia*

Canh-Dung Tran − *School of Mechanical and Electrical Engineering, University of Southern Queensland, Toowoomba, QLD 4350, Australia;* orcid.org/0000-0002-1011-4226

Hong-Quan Nguyen − *School of Engineering and Built Environment, Griffith University, Gold Coast, QLD 4215, Australia*

Tuan-Hung Nguyen − *School of Engineering and Built Environment, Griffith University, Gold Coast, QLD 4215, Australia*

Thanh Nguyen − *School of Mechanical and Electrical Engineering, University of Southern Queensland, Toowoomba, QLD 4350, Australia;* orcid.org/0000-0002-3213-6178

Tuan-Khoa Nguyen − *Queensland Micro and Nanotechnology Centre, Griffith University, Brisbane, QLD 4111, Australia;* orcid.org/0000-0003-1271-9576

Jarred W. Fastier-Wooller − *School of Engineering and Built Environment, Griffith University, Gold Coast, QLD 4215, Australia; School of Engineering, University of Tokyo, Tokyo 113-8656, Japan;* orcid.org/0000-0003-1119-2223

Toan Dinh − *School of Mechanical and Electrical Engineering, University of Southern Queensland, Toowoomba, QLD 4350, Australia*

Hoang-Phuong Phan − *School of Mechanical and Manufacturing Engineering, University of New South Wales, Sydney, NSW 2052, Australia;* orcid.org/0000-0002-1724-5667

Hang Thu Ta − *Queensland Micro and Nanotechnology Centre, Griffith University, Brisbane, QLD 4111, Australia; Australian Institute for Bioengineering and Nanotechnology, University of Queensland, Brisbane, QLD 4067, Australia; School of Environment and Science, Griffith University, Brisbane, QLD 4211, Australia;* orcid.org/0000-0003-1188-0472

Nam-Trung Nguyen − *Queensland Micro and Nanotechnology Centre, Griffith University, Brisbane, QLD 4111, Australia*

Dzung Viet Dao − *School of Engineering and Built Environment, Griffith University, Gold Coast, QLD 4215, Australia;* orcid.org/0000-0002-6348-0879

Complete contact information is available at:
https://pubs.acs.org/10.1021/acsami.3c02000

Notes

The authors declare no competing financial interest.

■ ABBREVIATIONS

EHDA, electrohydrodynamic atomization
PVDF, poly(vinylidene fluoride)
ES, electrospraying
AC, alternating current
SR, sphere radius
SEM, scanning electron microscope
DMEM/F12, Dulbecco's modified Eagle's medium/nutrient mixture F12
PFA, paraformaldehyde
DMF, *N*,*N*-dimethylformamide
ACE, acetone
FBS, fetal bovine serum (FBS)
HBSS, Hanks' balanced salt solution

■ REFERENCES

(1) Nikolaou, M.; Krasia, C. T. Electrohydrodynamic Methods for the Development of Pulmonary Drug Delivery Systems. *Eur. J. Pharm. Sci.* **2018**, *113*, 29−40.
(2) Pawar, A.; Thakkar, S.; Misra, M. A Bird's Eye View of Nanoparticles Prepared by Electrospraying: Advancements in Drug Delivery Field. *J. Controlled Release* **2018**, *286*, 179−200.
(3) Demoly, P.; Hagedoorn, P.; de Boer, A. H.; Frijlink, H. W. The Clinical Relevance of Dry Powder Inhaler Performance for Drug Delivery. *Respir. Med.* **2014**, *108*, 1195−1203.
(4) Zanen, P.; Go, L. T.; Lammers, J. W. J. The Optimal Particle Size for Parasympathicolytic Aerosols in Mild Asthmatics. *Int. J. Pharm.* **1995**, *114*, 111−115.
(5) Telko, M. J.; Hickey, A. J. Dry Powder Inhaler Formulation. *Respir. Care* **2005**, *50*, 1209−1227.
(6) Zhou, Q. T.; Tang, P.; Leung, S. S. Y.; Chan, J. G. Y.; Chan, H. K. Emerging Inhalation Aerosol Devices and Strategies: Where Are We Headed? *Adv. Drug Delivery Rev.* **2014**, *75*, 3−17.
(7) Kumar, N.; Gautam, V.; Kumar, V.; Maurya, P. K. Nanoparticle-Based Macromolecule Drug Delivery to Lungs. *Targeting Chronic Inflammatory Lung Dis. Using Adv. Drug Delivery Syst.* **2020**, 227−259.
(8) Rezk, A. R.; Ahmed, H.; Ramesan, S.; Yeo, L. Y. High Frequency Sonoprocessing: A New Field of Cavitation-Free Acoustic Materials Synthesis, Processing, and Manipulation. *Adv. Sci.* **2021**, *8*, No. 2001983.
(9) Rajapaksa, A.; Qi, A.; Yeo, L. Y.; Coppel, R.; Friend, J. R. Enabling Practical Surface Acoustic Wave Nebulizer Drug Delivery via Amplitude Modulation. *Lab Chip* **2014**, *14*, 1858−1865.
(10) Qi, A.; Friend, J. R.; Yeo, L. Y.; Morton, D. A. V.; McIntosh, M. P.; Spiccia, L. Miniature Inhalation Therapy Platform Using Surface Acoustic Wave Microfluidic Atomization. *Lab Chip* **2009**, *9*, 2184−2193.
(11) El-Sherbiny, I. M.; El-Baz, N. M.; Yacoub, M. H. Inhaled Nano -and Microparticles for Drug Delivery. *Global Cardiol. Sci. Pract.* **2015**, *2015*, No. 2.
(12) Hofstadler, S. A.; Sannes-Lowery, K. A. Applications of ESI-MS in Drug Discovery: Interrogation of Noncovalent Complexes. *Nat. Rev. Drug Discovery* **2006**, *5*, 585−595.
(13) Wleklinski, M.; Loren, B. P.; Ferreira, C. R.; Jaman, Z.; Avramova, L.; Sobreira, T. J. P.; Thompson, D. H.; Cooks, R. G. High Throughput Reaction Screening Using Desorption Electrospray Ionization Mass Spectrometry. *Chem. Sci.* **2018**, *9*, 1647−1653.
(14) Dolovich, M. B.; Dhand, R. Aerosol Drug Delivery: Developments in Device Design and Clinical Use. *Lancet* **2011**, *377*, 1032−1045.
(15) Yoo, J.-W.; Irvine, D. J.; Discher, D. E.; Mitragotr, S. Bio-Inspired, Bioengineered and Biomimetic Drug Delivery Carriers. *Nat. Rev. Drug Discovery* **2011**, *10*, 521−535.
(16) Zeleny, J. Instability of Electrified Liquid Surfaces. *Phys. Rev.* **1917**, *10*, 1−6.
(17) Gan, Y.; Li, H.; Jiang, Z.; Chen, X.; Luo, Y.; Tong, Y.; Shi, Y.; Jiang, X. An Experimental Investigation on the Electrospray Characteristics in a Meso-Scale System at Different Modes. *Exp. Therm. Fluid Sci.* **2019**, *106*, 130−137.
(18) Steipel, R. T.; Gallovic, M. D.; Batty, C. J.; Bachelder, E. M.; Ainslie, K. M. Electrospray for Generation of Drug Delivery and Vaccine Particles Applied in Vitro and in Vivo. *Mater. Sci. Eng., C* **2019**, *105*, No. 110070.
(19) Xu, J.; Li, K.; Liu, M.; Gu, X.; Li, P.; Fan, Y. Studies on Preparation and Formation Mechanism of Poly(Lactide-Co-Glycolide) Microrods via One-Step Electrospray and an Application for Drug Delivery System. *Eur. Polym. J.* **2021**, *148*, No. 110372.
(20) Chen, C.; Wang, Y.; Zhang, D.; Wu, X.; Zhao, Y.; Shang, L.; Ren, J.; Zhao, Y. Natural Polysaccharide Based Complex Drug Delivery System from Microfluidic Electrospray for Wound Healing. *Appl. Mater. Today* **2021**, *23*, No. 101000.
(21) Yuan, S.; Lei, F.; Liu, Z.; Tong, Q.; Si, T.; Xu, R. X. Coaxial Electrospray of Curcumin-Loaded Microparticles for Sustained Drug Release. *PLoS One* **2015**, *10*, No. e0132609.
(22) Ijsebaert, J. C.; Geerse, K. B.; Marijnissen, J. C. M.; Lammers, J. W. J.; Zanen, P. Electro-Hydrodynamic Atomization of Drug Solutions for Inhalation Purposes. *J. Appl. Physiol.* **2001**, *91*, 2735−2741.
(23) Mustika, W. S.; Hapidin, D. A.; Saputra, C.; Munir, M. M. Dual Needle Corona Discharge to Generate Stable Bipolar Ion for Neutralizing Electrosprayed Nanoparticles. *Adv. Powder Technol.* **2021**, *32*, 166−174.
(24) Ciach, T. Microencapsulation of Drugs by Electro-Hydro-Dynamic Atomization. *Int. J. Pharm.* **2006**, *324*, 51−55.
(25) Borra, J. P.; Camelot, D.; Chou, K. L.; Kooyman, P. J.; Marijnissen, J. C. M.; Scarlett, B. Bipolar Coagulation for Powder Production: Micro-Mixing inside Droplets. *J. Aerosol Sci.* **1999**, *30*, 945−958.
(26) Almekinders, J. C.; Jones, C. Multiple Jet Electrohydrodynamic Spraying and Applications. *J. Aerosol Sci.* **1999**, *30*, 969−971.
(27) Fernandez de la Mora, J.; Barrios-Collado, C. A Bipolar Electrospray Source of Singly Charged Salt Clusters of Precisely Controlled Composition. *Aerosol Sci. Technol.* **2017**, *51*, 778−786.
(28) Borra, J. P.; Camelot, D.; Marijnissen, J. C. M.; Scarlett, B. A New Production Process of Powders with Defined Properties by Electrohydrodynamic Atomization of Liquids and Post-Production Electrical Mixing. *J. Electrost.* **1997**, *40*−*41*, 633−638.
(29) Dau, V. T.; Terebessy, T. Electrostatic Spraying Apparatus, and Current Control Method for Electrostatic Spraying Apparatus. US9,937,508, Feb, 2014.
(30) Jaworek, A.; Sobczyk, A. T.; Krupa, A. Electrospray Application to Powder Production and Surface Coating. *J. Aerosol Sci.* **2018**, *125*, 57−92.
(31) Meesters, G. M. H.; Vercoulen, P. H. W.; Marijnissen, J. C. M.; Scarlett, B. Generation of Micron-Sized Droplets from the Taylor Cone. *J. Aerosol Sci.* **1992**, *23*, 37−49.
(32) Dau, V. T.; Dinh, T. X.; Tran, C. D.; Terebessy, T.; Duc, T. C.; Bui, T. T. Particle Precipitation by Bipolar Corona Discharge Ion Winds. *J. Aerosol Sci.* **2018**, *124*, 83−94.
(33) Morozov, V. N. Generation of Biologically Active Nano-Aerosol by an Electrospray-Neutralization Method. *J. Aerosol Sci.* **2011**, *42*, 341−354.
(34) Carrasco-Munoz, A.; Barbero-Colmenar, E.; Bodnár, E.; Grifoll, J.; Rosell-Llompart, J. Monodisperse Droplets and Particles by Efficient Neutralization of Electrosprays. *J. Aerosol Sci.* **2022**, *160*, No. 105909.
(35) Demekhin, E.; Polyanskikh, S.; Ramos, A. Taylor Cones in a Leaky Dielectric Liquid under an Ac Electric Field. *Phys. Rev. E* **2011**, *84*, No. 035301.

(36) Chetwani, N.; Cassou, C. A.; Go, D. B.; Chang, H.-C. Frequency Dependence of Alternating Current Electrospray Ionization Mass Spectrometry. *Anal. Chem.* **2011**, *83*, 3017−3023.
(37) Dau, V. T.; Nguyen, T.-K.; Dao, D. V. Charge Reduced Nanoparticles by Sub-KHz Ac Electrohydrodynamic Atomization toward Drug Delivery Applications. *Appl. Phys. Lett.* **2020**, *116*, No. 023703.
(38) Yeo, L. Y.; Lastochkin, D.; Wang, S. C.; Chang, H. C. A New Ac Electrospray Mechanism by Maxwell-Wagner Polarization and Capillary Resonance. *Phys. Rev. Lett.* **2004**, *92*, No. 133902.
(39) Yeo, L. Y.; Gagnon, Z.; Chang, H. C. AC Electrospray Biomaterials Synthesis. *Biomaterials* **2005**, *26*, 6122−6128.
(40) Kebarle, P.; Peschke, M. On the Mechanisms by Which the Charged Droplets Produced Byelectrospray Lead to Gas Phase Ions. *Anal. Chim. Acta* **2000**, *406*, 11−35.
(41) Dau, V. T.; Vu, H. T.; Tran, C.; Nguyen, T. V.; Nguyen, T.-K.; Dinh, T.; Phan, H.; Shimizu, K.; Nguyen, N.; Dao, D. V. Electrospray Propelled by Ionic Wind in a Bipolar System for Direct Delivery of Charge Reduced Nanoparticles. *Appl. Phys. Express* **2021**, *14*, No. 055001.
(42) Correia, D. M.; Gonçalves, R.; Ribeiro, C.; Sencadas, V.; Botelho, G.; Ribelles, J. L. G.; Lanceros-Méndez, S. Electrosprayed Poly(Vinylidene Fluoride) Microparticles for Tissue Engineering Applications. *RSC Adv.* **2014**, *4*, 33013−33021.
(43) Vu, T.-H.; Nguyen, H. T.; Fastier-Wooller, J. W.; Tran, C.-D.; Nguyen, T.-H.; Nguyen, H.-Q.; Nguyen, T.; Nguyen, T.-K.; Dinh, T.; Bui, T. T.; Zhong, Y.; Phan, H.-P.; Nguyen, N.-T.; Dao, D. V.; Dau, V. T. Enhanced Electrohydrodynamics for Electrospinning a Highly Sensitive Flexible Fiber-Based Piezoelectric Sensor. *ACS Appl. Electron. Mater.* **2022**, *4*, 1301−1310.
(44) Dau, V. T.; Dinh, T. X.; Bui, T. T.; Tran, C. D.; Phan, H. T.; Terebessy, T. Corona Based Air-Flow Using Parallel Discharge Electrodes. *Exp. Therm. Fluid Sci.* **2016**, *79*, 52−56.
(45) Peek, F. W. *Dielectric Phenomena in High Voltage Engineering*; McGraw-Hill Book Company, Incorporated, 1920.
(46) Robinson, M. Movement of Air in the Electric Wind of the Corona Discharge. *Trans. Am. Inst. Electr. Eng., Part 1* **1961**, *80*, 143−150.
(47) Tarabová, B.; Lukeš, P.; Janda, M.; Hensel, K.; Šikurová, L.; Machala, Z. Specificity of Detection Methods of Nitrites and Ozone in Aqueous Solutions Activated by Air Plasma. *Plasma Process. Polym.* **2018**, *15*, No. 1800030.
(48) Guo, Y.; Li, S.; Wu, Z.; Zhu, K.; Han, Y.; Wang, N. Interaction between Electrospray Using Ionic Liquid and Simultaneous Corona Discharge under Positive and Negative Polarity. *Phys. Plasmas* **2019**, *26*, No. 073511.
(49) Zhang, Y.; Liu, L.; Chen, Y.; Ouyang, J. Characteristics of Ionic Wind in Needle-to-Ring Corona Discharge. *J. Electrost.* **2015**, *74*, 15−20.
(50) Yamada, K. An Empirical Formula for Negative Corona Discharge Current in Point-Grid Electrode Geometry. *J. Appl. Phys.* **2004**, *96*, 2472−2475.
(51) Kip, A. F. Onset Studies of Positive Point-to-Plane Corona in Air at Atmospheric Pressure. *Phys. Rev.* **1939**, *55*, 549.
(52) Dau, V. T.; Bui, T. T.; Tran, C. D.; Nguyen, T. V. T. K.; Nguyen, T. V. T. K.; Dinh, T.; Phan, H. P.; Wibowo, D.; Rehm, B. H. A.; Ta, H. T.; Nguyen, N. T.; Dao, D. V. In-Air Particle Generation by on-Chip Electrohydrodynamics. *Lab Chip* **2021**, *21*, 1779−1787.
(53) Megelski, S.; Stephens, J. S.; Chase, D. B.; Rabolt, J. F. Micro- and Nanostructured Surface Morphology on Electrospun Polymer Fibers. *Macromolecules* **2002**, *35*, 8456−8466.
(54) Zhang, H.; Xu, R.; Yin, Z.; Yu, J.; Liang, N.; Geng, Q. Drug-Loaded Chondroitin Sulfate Microspheres Generated from Microfluidic Electrospray for Wound Healing. *Macromol. Res.* **2022**, *30*, 36−42.
(55) Chen, H. C.; Tsai, C. H.; Yang, M. C. Mechanical Properties and Biocompatibility of Electrospun Polylactide/Poly(Vinylidene Fluoride) Mats. *J. Polym. Res.* **2011**, *18*, 319−327.
(56) Rodrigues, M. T.; Gomes, M. E.; Mano, J. F.; Reis, R. L. β-PVDF Membranes Induce Cellular Proliferation and Differentiation in Static and Dynamic Conditions. *Mater. Sci. Forum* **2008**, *587*−*588*, 72−76.
(57) de Charras, Y. L.; Bertin, D. E.; Ramírez-Rigo, M. V. Influence of the Valve on the Performance of Two Cylindrical Valved Holding Chambers. *Powder Technol.* **2022**, *414*, No. 118094.
(58) Barry, P. W.; O'Callaghan, C. The Optimum Size and Shape of Spacer Devices for Inhalational Therapy. *J. Aerosol Med.* **1995**, *8*, 303−305.
(59) Martynenko, A.; Astatkie, T.; Defraeye, T. The Role of Convection in Electrohydrodynamic Drying. *J. Food Eng.* **2020**, *271*, No. 109777.
(60) Angkawinitwong, U.; Courtenay, A. J.; Rodgers, A. M.; Larrañeta, E.; Mccarthy, H. O.; Brocchini, S.; Donnelly, R. F.; Williams, G. R. A Novel Transdermal Protein Delivery Strategy via Electrohydrodynamic Coating of PLGA Microparticles onto Microneedles. *ACS Appl. Mater. Interfaces* **2020**, *12*, 12478−12488.
(61) Gañán-Calvo, A. M.; López-Herrera, J. M.; Herrada, M. A.; Ramos, A.; Montanero, J. M. Review on the Physics of Electrospray: From Electrokinetics to the Operating Conditions of Single and Coaxial Taylor Cone-Jets, and AC Electrospray. *J. Aerosol Sci.* **2018**, *125*, 32−56.
(62) Park, I.; Hong, W. S.; Kim, S. B.; Kim, S. S. Experimental Investigations on Characteristics of Stable Water Electrospray in Air without Discharge. *Phys. Rev. E* **2017**, *95*, 1−8.
(63) Boda, S. K.; Li, X.; Xie, J. Electrospraying an Enabling Technology for Pharmaceutical and Biomedical Applications: A Review. *J. Aerosol Sci.* **2018**, *125*, 164−181.
(64) Zhu, L.; Li, M.; Liu, X.; Jin, Y. Drug-Loaded PLGA Electrospraying Porous Microspheres for the Local Therapy of Primary Lung Cancer via Pulmonary Delivery. *ACS Omega* **2017**, *2*, 2273−2279.

Supporting information

Charge-reduced particles via self-propelled electrohydrodynamic atomisation for drug delivery applications

Trung-Hieu Vu,[1] Sharda Yadav,[2] Canh-Dung Tran,[3] Hong-Quan Nguyen,[1] Tuan-Hung Nguyen,[1] Thanh Nguyen,[3] Tuan-Khoa Nguyen,[2] Jarred W. Fastier-Wooller,[1,4] Toan Dinh,[3] Hoang-Phuong Phan,[5] Hang Thu Ta,[2,6,7] Nam-Trung Nguyen,[2] Dzung Viet Dao,[1] Van Thanh Dau[8]*

[1]School of Engineering and Built Environment, Griffith University, Gold Coast, 4215, AUSTRALIA

[2]Queensland Micro and Nanotechnology Centre, Griffith University, Brisbane, 4111, AUSTRALIA

[3]School of Mechanical and Electrical Engineering, University of Southern Queensland, Toowoomba, 4350, AUSTRALIA

[4]School of Engineering, The University of Tokyo, Tokyo, 113-8656, JAPAN

[5]School of Mechanical and Manufacturing Engineering, The University of New South Wales, Sydney, 2052, AUSTRALIA

[6]Australian Institute for Bioengineering and Nanotechnology, The University of Queensland, Brisbane, 4067, AUSTRALIA

[7]School of Environment and Science, Griffith University, Gold Coast, 4215, AUSTRALIA

[8]Centre for Catalysis and Clean Energy, Griffith University, Gold Coast, 4215, AUSTRALIA

E-mail: trunghieu.vu@griffithuni.edu.au

The PDF file includes

Section S1: Charge reduction in ES particles via ion wind.

Corona discharge has always been an attractive approach to reduce charge in ES particles and neutralise them due to applicability of implementation. In principle, reducing charge in ES particles requires constant supply of ions so the particles can reach the equilibrium state. Techniques such as radio-ionisation, photonionisation, or X-ray irradiation are also proven to be capable of producing ions to suit this purpose [1]. However, the requirements of bulky equipment, complex components, control system, safety concerns, cost, as well as limited materials prevent them from being widely applied. On the other hand, corona discharge is an uncomplicated technique which can reduce charge in ES particles. Mustika et al. [2] implemented a system with two chambers, one generates highly charged ES particles and the other neutralises them by generating bipolar ions (ions of both polarities) from a dual needle setup. The experiment showed success in reducing charge in ES particles, but the system displays significant complexity in the design. An external gas supply is placed in the spray chamber (the chamber where ES occurs) to guide the flow of particles toward the charge reduction chamber (the chamber where dual needle setup is placed). In the latter chamber, the two needles powered externally produce bipolar ions which reduce the charge in ES particles. Despite the simple concept, this system requires external sub-systems and power supplies whereas the neutralisation process is separate from generation of ES particles. This shows the need for a simple design which can establish simultaneous neutralisation and constant momentum to drive ES particles.

In this research, we designed and experimented with a corona discharge system while fabricating ES particles. Our system uses only one power source and exploits the corona discharge to neutralise the ES particles. The experimental setup in Fig. S1A describes the electrical system. When high voltage is applied, the ES particles are generated and charged with positive ions. The ionisation of air molecules near the vicinity of the pin cause ion wind which is full of negative ions. The interaction between ion wind and plume of droplets eventually causes recombination of ions. The collisions between two ions of opposite polarities result in charge reduced particles, i.e., electroneutral particles. In Fig.S1, experimental setup demonstrates the visualisation of ion wind. A smoke source is placed under the nozzle so the flow of smoke can visualise the existence of ion wind. Without the existence of ion wind, smoke can be observed as seen in Fig. S1B, flowing oppositely to the gravitation. When ion wind presents, plume of smoke is propelled by the momentum of air as seen in Fig. S1 C. A velocity probe is placed 5 mm from the nozzle to measure velocity of ion wind and data is presented in the main manuscript. The momentum from ion wind propels the particles to target.

Our device maintains a state of charge balance, where the charge carried by the atomised droplets from the nozzle is equal to the charge in the ion wind generated from the pin. The voltage applied between the two electrodes can be used to control the charge in the ion wind, which can be measured using an aerosol electrometer (TSI, model 3068B). The device is placed in an enclosed container, and the electrometer measures the charge in the generated particles at the pin. The measurement point is 1 cm downward from the pin to determine the charge in the ion wind. The electrometer draws particles and droplets at a rate of 10 litres per minute (LPM). The experimental setup is presented in Fig. S2A. A lower voltage results in a greater negative charge generated by the ion wind. For instance, when spraying IPA at a constant rate of 0.5 ml/hr, increasing the voltage from 4 to 4.5 kV results in a decrease in average charge from -1.02 to -10.36 pA. The graph in Fig. S2B presents the charge in the ion wind as the voltage increases. The charge in the ion wind can be controlled by simply adjusting the voltage, providing a method for controlling the neutralisation process in our device.

We investigated the charge reduction in particles and droplets when they are negatively charged. Specifically, the nozzle was connected to the negative (-) and the pin was connected to the positive (+) poles of the power source. We employed a 5 wt% PVDF solution and measured the current in the

resulting plume of particles. The voltage to maintain a stable spray was 6.22 kV and the spray current was 2.10 µA at a flow rate of 0.5 ml/hr. The average charge of sprayed PVDF particles, measured by electrometer is 4.55 pA (Fig. S2C). This charge is only a fraction of the total spray current of 2.10 µA (2.10×10^6 pA pA) and is a result of the interaction between negative particles and positive ion wind. This demonstrates effective charge reduction regardless of whether the pin is positive or negative, as shown in Fig. S2C.

The neutrality can be quantified by measuring the total net charge in the generated particles at 10 cm downstream from the nozzle. In our experiments, we used PVDF 5% solution sprayed at a flow rate of 0.5 ml/hr and 5 kV to maintain a stable Taylor cone. The average charge in generated particles is -949 fA at 10 cm (Fig.S2D). This value is several times lower than the current spray 4.1 µA (4.1×10^9 fA) between the two electrodes. In conventional methods, the current between the electrodes equal to the current in the generated particles.

We also conducted experiments to visualise the neutrality of the generated particles by comparing them with a conventional electrospray method. The conventional method uses a point-plane configuration, where the generated particles are highly charged and can easily be attracted to a grounded object placed between the two electrodes, typically a metal ring downstream from the nozzle where voltage is applied (Fig. S3). In the point-ring configuration, the ring attracts all the positively charged particles as it is grounded. However, in our system, the particles can bypass the ring as their charge is reduced and they are not attracted to the ring. PVDF 5 wt% was chosen to demonstrate the charge reduction in both configurations. In Fig. S3, the particles in the conventional method are attracted to the ring and do not reach the plane, which is the negative electrode. In our configuration, particles can be seen passing the ring and some flying back to the ring. This indicates that the charge has been reduced but not completely eliminated. Further optimisation and investigation can be carried out to improve the neutrality of the generated particles.

Section S2: Controllability over formation of particles and fibres.

Section S2.1:Self-propelled EHDA as an alternative for *produc*tion of *polymer fibre*

Electrospraying and electrospinning are two hydrodynamic techniques which are distinguished from each other by the formation of their products [3]. Electrospraying allows formation of particulate products whereas electrospinning facilitates fibres [4]. This contributing difference between the two techniques is caused mostly by concentration of polymeric content in the solution. In this research, we have formulated PVDF solutions at various concentrations while the ratio of solvent is kept constant. This indicates uniformity across experimental results. Polyvinylidene fluoride (PVDF) powder (M_w≈ 534,000, Sigma-Aldrich) is dissolved in a 4:1 ratio mixture of N,N- Dimethylformamide > 99a% (DMF, Sigma-Aldrich) and Acetone ≥ 99.5% (ACE, Sigma-Aldrich) at various of concentrations of 5 wt%, 10 wt%, 15 wt%, and 20 wt%. Solution is prepared by stirring vigorously at 40°C for 4 hours, until solution reaches consistent transparency and homogeneity. Conducting experiments with solutions of increasing polymer concentration investigates the formation of final products fabricated via our system and is discussed in our paper.

Conventional electrospinning also fabricates highly charged fibres collected on grounded static collector [5]. Fibres are collected on a metal substrate such as aluminium foil or conductive mesh before treatment for applications. This implies conventional electrospinning is not suitable for direct collection of fibres. In contrast, our approach allows direct collect as the generation and formation of fibres no longer relies on collector. Fig. S8 shows particles and fibres collected on substrates of various properties. All substrates are placed from a collecting distance of 5 cm to the nozzle, unaffected by

the electric field between the electrodes. Significantly, thin strands of fibres from PVDF 15 wt% collected on paper substrate suggests possible formation of uniform fibres by tuning the experimental parameters. In other words, this feature presents the substantial advancement to conventional electrospinning. Our self-propelled system disregards the need for a collector. Instead, the products including particles and fibres can be directly deposited onto surfaces of various properties as long as they provide sufficient adhesion.

Section S2.2: Self-propelled EHDA as an effective method for production of particles

We conducted experiments to determine the size distribution of particles in two modes: single-jet and multi-jet. The experiments were performed in an enclosed container that was connected to an optical particle sizer (OPS, TSI 3330) and the measurement point was 10 cm downstream from the nozzle tip. We sprayed IPA solution at a rate of 0.5 ml/hr with voltages of 4 kV and 5.3 kV to produce single-jet and multi-jet modes, respectively. The majority of particles generated by both single-jet and multi-jet modes were within the size range of 0.300-0.579 µm. However, multi-jet mode generated particles as large as 5 µm. The graph in Fig. S5 shows distribution of generated IPA particles. The single-jet mode generates approximately 10,000 particles per second, while the multi-jet mode generates approximately 12,000 particles per second. This result is in the same order with particle generating rate reported in previous literature, and the equipment limitations prevented the counting of particles smaller than 0.3 µm[1] . The size distribution also indicates that multi-jet mode can produce more particles with larger sizes than single-jet. This result aligns well with previous literature in which cone jet mode can produce particles with lower mean diameter and are more monodisperse than multi jet mode in electrospray[2,3]. Advantage of electrospray lies in the production of uniform particles of uniform particles, so optimisation of spraying conditions will be investigated further in future work.

Previous research has shown that EHDA in its conventional form can successfully atomise a wide range of solutions, including polymer solutions, drug solutions, and even biological solutions such as proteins and DNA[6–8]. In our study, we were able to generate micro and nano particles from various polymers, namely polyethylene (PU), polycaprolactone (PCL), and polyvinylidene fluoride (PVDF). The spray conditions and morphologies of these different polymers are presented in SEM images in Fig. S6. It is worth noting that the spraying parameters, such as voltage, solution concentration, nozzle size, collecting distance, and others, play a significant role in the controllability of the final products. Therefore, refinement and optimisation are required for each specific solution to achieve the desired outcomes. Further research will be carried out to develop and adapt optimisation.

Two common solutions with similar surface tension were used to demonstrate how the size of generated particles is influenced by different properties in the solution. The device was placed in an enclosed container connected to an Optical Particle Sizer (OPS) (TSI 3330, 1 LPM) to analyse the size distribution of particles of Isopropyl Alcohol (IPA) and Di(propylene glycol) methyl ether (DPM) in the air. IPA (99.5%, Sigma-Aldrich) has the following properties: surface tension $\gamma \approx 20.8$ mN/m, density $\rho \approx 0.785$ g/ml, viscosity $\mu \approx 1.66$ mPas, conductivity $K \approx 6$ µS/m, vapour pressure = 40 mmHg, and relative permittivity $\varepsilon \approx 18.6$. DPM (>99%, Sigma-Aldrich) has the following properties: surface tension $\gamma \approx 28.7$ mN/m, density $\rho \approx 0.951$ g/ml, viscosity $\mu \approx 3.7$ mPas, and vapour pressure =0.4 mmHg. The size distribution of airborne particles of the two solutions is presented in the Fig. S5B. The two solutions have similar surface tensions but differ in terms of their vapor pressure values, resulting in generation of larger particles from DPM. The choice of solution can impact the generation and formation of particles significantly.

Our configuration showed successful fabrication and delivery of particles at distance of 10 cm. We optimised the spraying parameters for fabrication PVDF particles at 10 cm to deliver to cells. We

successfully fabricated and delivered PVDF 5 wt% with flow rate of 0.5 ml/hr, voltage of 4.7 kV, onto fixed cells at 10 cm from the device. The average size is 1.8 µm with standard deviation of 0.36 µm among 400 particles were analysed. The parameters are the same as spraying conditions in "Single-step delivery of particles onto cells" in the manuscript. Figure S7 shows the morphology and size distribution of particle collected at 10 cm from the device.

Section S3: Self-propelled EHDA with respect to atomisation and drug delivery technologies

Our self-propelled EHDA combines corona discharge and atomisation to produce nanosized electroneutral droplets and particles. Drug delivery is a typical application where particles must be neutralised before deposition. Therefore, we concisely discuss self-propelled EHDA in the context of atomisation and drug delivery technologies.

Nebuliser is a common device used for pulmonary drug delivery that can break up jet of fluid into droplets suitable for inhalation. When in use, the nebuliser bowl contains drug in aqueous solution whereas compressed air is applied to the inlet and escapes via a narrow orifice. The Venturi effect causes the solution to be drawn up, collapsing with the nebuliser walls or baffles, and fine droplets are carried out of the nebuliser and inhaled by a patient. The dispersing force is the contributing factor to the generation of droplets [9]. However, the size of droplets and particles in commercial devices can still be optimized. For pulmonary drug delivery, the range size for optimal drug absorption is between 3 – 5 µm. Farzal *et al.* conducted a comparative study and found that the droplets output from readily available nebulisers and the majority of droplets are within the 7 – 14 µm [10]. At this size range, previous studies suggest drug droplets and particles are not able to reach deep lungs, leading to ineffective treatment [11,12]. Drawbacks of nebuliser includes time of use and portability. For each use, the patient needs to sit still for up to 15 minutes to inhale the atomized medication. The required accessories and components of typical nebulisers make them difficult to be carried around and regular maintenance is needed for infection control. Even though battery-operated nebulisers are available, challenges such as low efficiency, or medication loss still remain [13].

Inhaler is widely used in pulmonary treatment due to its size, portability, and effectiveness. Inhalers incorporate a consumable canister containing aerosol medicine to be consumed inhalation. There are two common types of inhalers: metered-dose inhalers (MDI), and dry powder inhalers (DPI) [9,13,14]. For MDI, drug is dissolved or suspended in the propellent under high pressure. When activated, drug and propellant is released from the canister by pressurized air, travelling through patient's airways. For DPI, drug is available in dry powder and is activated by patient's breathing action instead of pressure as MDI. Generally, DPIs are more complicated than MDIs and offer higher deposition of aerosolised drug particles [9]. However, previous literature suggests that inhalers face challenges in practical use [15]. Both inhalers require coordination from patients for effective treatment. In the case of DPI, patient needs to provide sufficient inspiration in the lung up to 30 L/min. Furthermore, atomisation via inhaler is more capable of delivering drug to the upper airways instead of distal airways. This depends on various factors such as particle size, choice of propellent, pressurized meter, etc.

In the field of nebulisation, surface acoustic wave (SAW) and Hybrid Resonant Acoustic (HYDRA) are other methods of creating particles without charge. These methods utilise vibration on the surface of a platform to nebulise droplets of liquid. To achieve this, a series of complicated process including UV photolithography, wet etching, and sputtering deposition is required to produce the transducer which is the heart of a SAW device. Furthermore, SAW only nebulises without delivering the fabricated mist of droplets. The momentum in fabricated particles and droplets depends on transfer of energy from the device onto the liquid and cannot be controlled without a subsystem such as a fan. In contrast, our device is developed upon the simplicity of conventional ES and do not require complex

manufacturing. Another advantage lies within the charge balance nature of the system. Since the device is supplied by only one source, the charge in the generated ion wind must be equal to the charge in the plume of particles. Thus, the propulsion from ion wind to assist and convey particles always coexist with the nebulisation of liquid. In other words, the neutralisation and delivery of particles always happen simultaneous whenever sufficient voltage is applied between the two electrodes (nozzle and pin). In term of power consumption, our device uses 0.09 W at optimal conditions while the SAW was reported to consume more than 4.5 W at the same flow rate of 1.5 ml/hr [16].

To achieve electroneutral particles in electrohydrodynamic, research has focused on various approaches. For applications with direct current, researchers apply additional system to neutralise generated particles or droplets. Morozov installed a second nozzle in a chamber and generated oppositely charged ions from volatile solvent to efficiently reduce charge in aerosol particles [17]. Recently, Carrasco-Munoz *et al* used one ES and one unipolar ion generation system [18] neutralise the ES particles, prevent the Coulombic instabilities in jet formation, and produce monodisperse polystyrene as well as curcumin-loaded particles. Alternatively, several alternating current (AC) EHDA approaches have been reported to overcome the charge reduction problem in ES. Similar to conventional ES, this method utilises high voltage between the capillary and collector to produce particles. However, this approach requires a supply voltage with alternating frequency to apply the electric field between the emitter and collector. Hence, the performance of AC EHDA highly depends on the operating frequency. For example, high frequency AC (10 kHz - 10 MHz) can produce micron-sized particles at resonating meniscus which is essentially different from normal DC setup [19,20].

In regard to drug delivery for pulmonary application, our self-propelled EHDA demonstrates an improvement in particles generation which has high potential for effective treatment. First, our self-propelled EHDA is capable of fabricating particles within suitable 3 – 5 μm size range. The suitable size range allows particles to reach lung with higher efficiency than inhalers and nebuliser. Second, our approach can simultaneously deliver the particles to targeted area with the generation of ion wind. Unlike inhalers, the delivery of particles does not depend on the compressed air as in MDIs or inhalation action as in DPIs. Instead, the droplets and particles are delivered via the ion wind's momentum. Third, the electroneutral particles indicate a great potential for our system to be used as inhalational device. Due to the neutralisation of corona discharge in ion wind, fabricated particles are at equilibrium state and can be inhaled safely and do not get lost along the airways. Loading particles with drug has been an interest research direction in electrohydrodynamic [21,22]. Drug can be added directly to the spraying solution and loaded particles can be collected for drug delivery systems. In the future, we will further optimise the system to further investigate the potential of this approach in drug delivery and biomedical applications. As such, our self-propelled EHDA combines effective size range, simultaneous delivery, good electroneutrality, and cell compatibility as shown in the main manuscript, and therefore open a new approach for effective drug delivery for pulmonary treatment.

We successfully demonstrated the capability of our device to generate and deliver particles directly onto cells. Breast cancer cells exhibit rapid and aberrant growth compared to healthy cells, as they do not stop dividing even when sufficient in number. Thus, for ease of observation, we chose breast cancer cells as our target cells, as they can be easily monitored. Our objective was to refine the spraying technique and highlight its potential in delivering biocompatible polymers onto living cells safely. The findings of our study indicate the promising application of this method, with a relatively simple optimisation process. Correia et al. conducted a viability test with MC3T3-E1 cells (derived from mouse calvaria) and found that electrosprayed PVDF particles can provide a suitable environment for cell growth [23]. Future studies will experiment with a wider range of materials and cell lines.

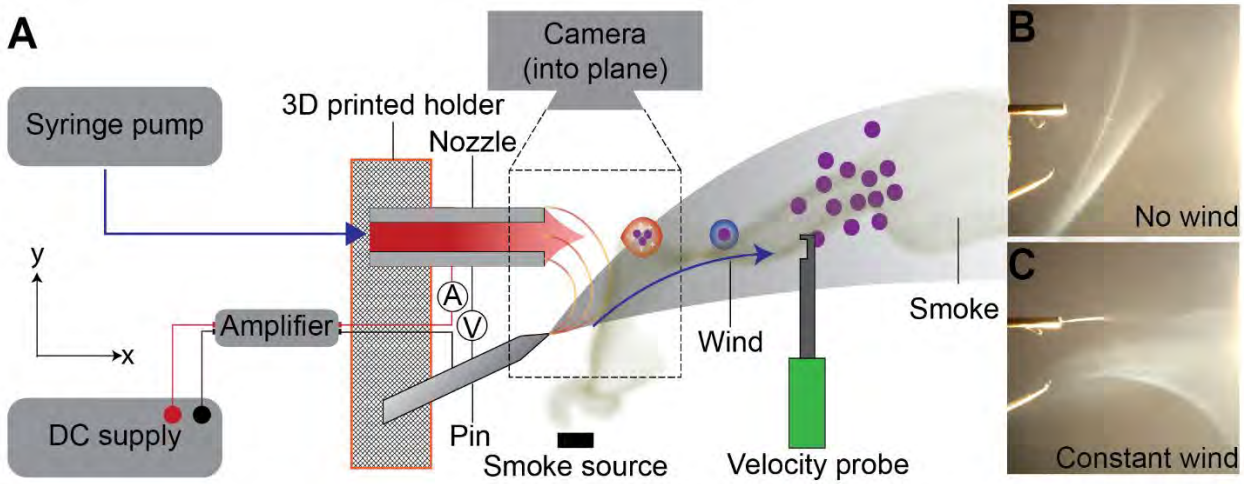

Fig S1. Schematic of experimental setup. (**A**) Experimental setup with smoke for visualisation purpose and velocity probe for velocity measurement. When there is no wind, the direction of smoke is upward as seen in (B). As the process is stable, the smoke visualises the movement of ion wind as seen in (C). The velocity probe is placed 5 mm away from the nozzle tip to measure velocity. During velocity measurement, no liquid was used to ensure only ion wind velocity is recorded. (**B-C**) Experimental images displaying how smoke visualises the system with and without ion wind.

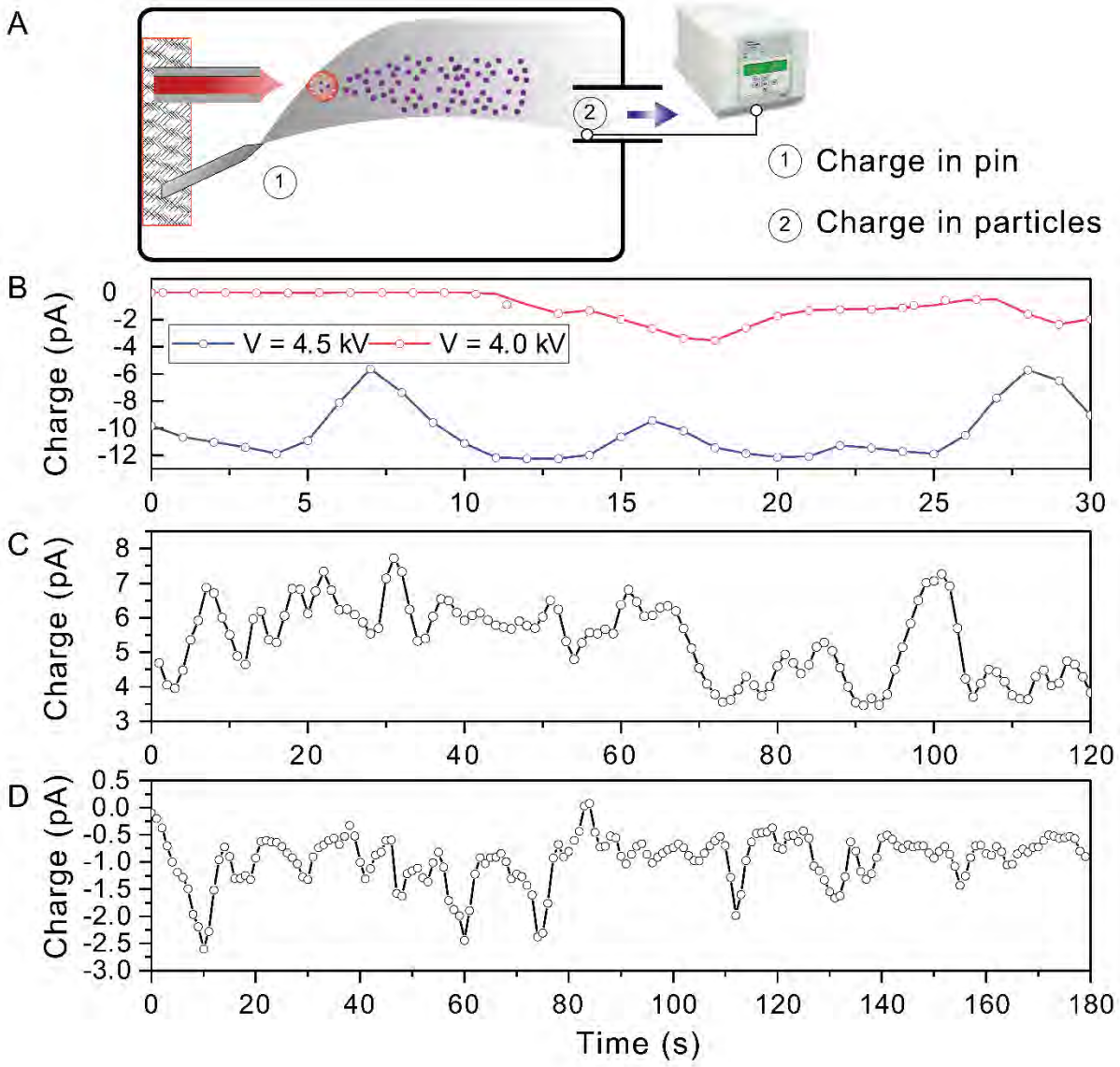

Fig S2. Charge measurement. (**A**) Experiment setup with aerosol electrometer at 2 positions. (**B**) Control of ion wind at position (1) at 4 kV and 4.5 kV. (**C**) Charge in ion wind when pin is positive (+). (D) Charge in generated particles from PVDF 5 wt% collected at position (2).

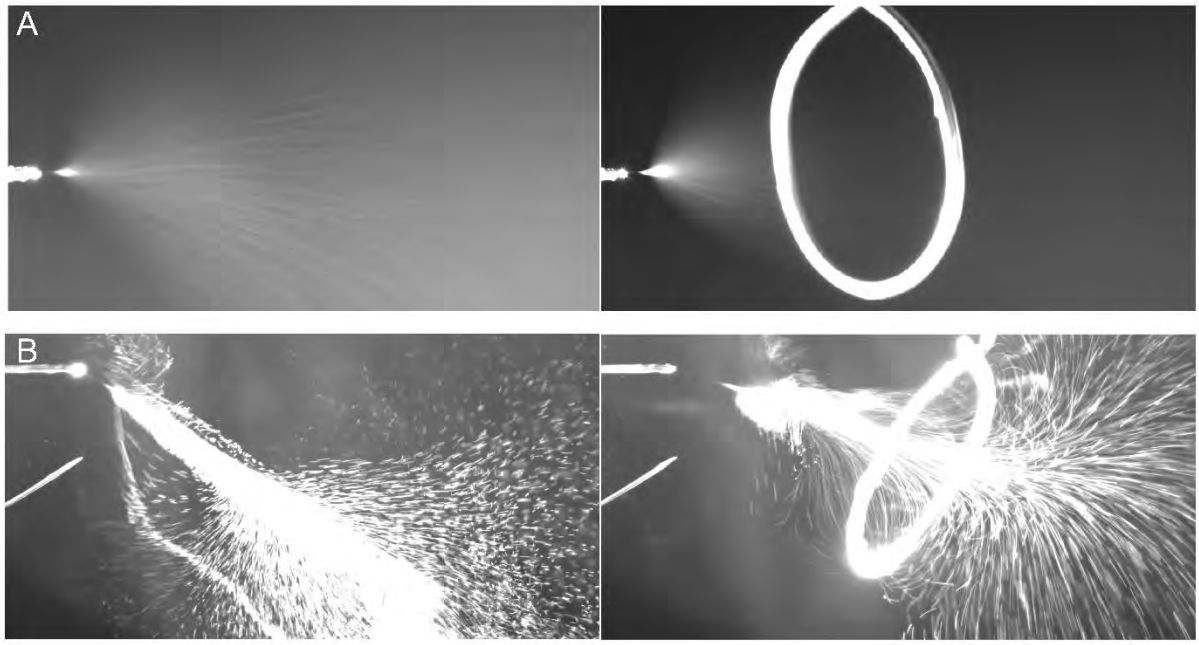

Fig S3. Visualisation of charge-reduced particles. (**A**) Generated particles in point-plane configuration in which PVDF particles are attracted to the ring placed between the two electrodes, the nozzle electrode is connected to positive voltage, the plane electrode is grounded and is on the right of the figure (not shown). (**B**) Generated particles in self-propelled EHDA in which PVDF particles can fly pass the metal ring due to charge reduction.

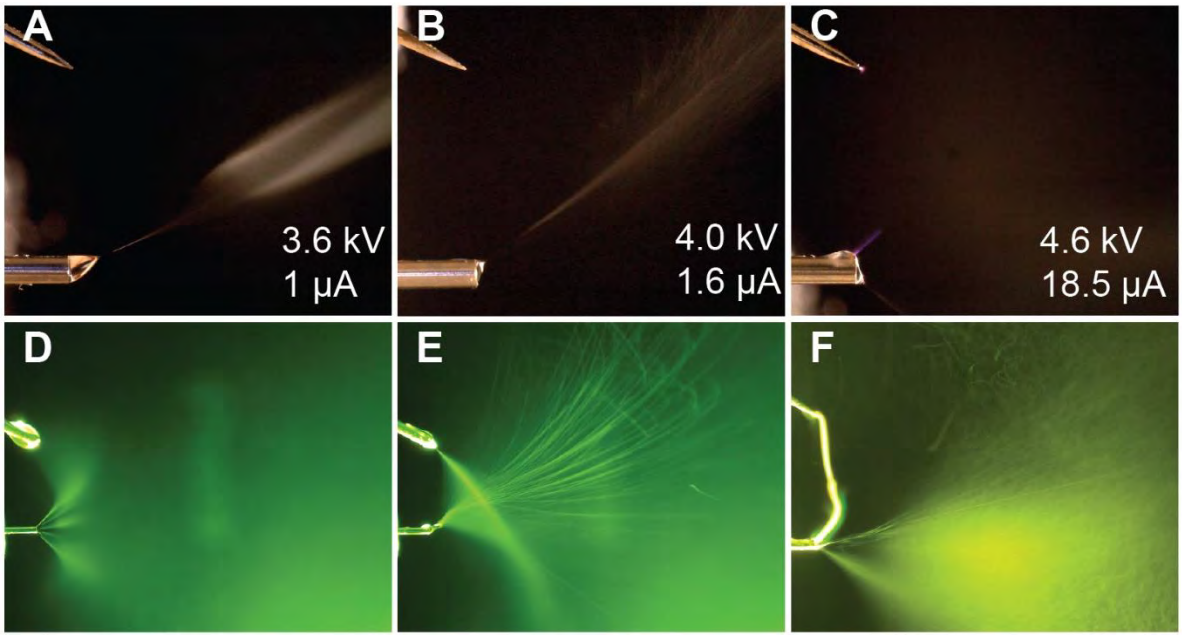

Fig S4. Spraying behaviour as voltage increases and destabilisation in spraying. due to accumulated droplet. (**A-C**) Spraying behaviour and current reading as voltage increases when the pin is sharp ($SR \approx 30$ μm) Taylor cone can be seen in (A) as well as tilted cone in (B). Corona discharge can be seen in (C) with a raise in current which can eventually develop into sparkling between two electrodes. (**D-E**) Spraying behaviour as voltage increases for a blunt pin ($SR \approx 130$ μm). The geometry of the pin prevents its from generating ion to neutralise and blow the plum of droplets. Instead, the plume of

droplets is attracted to the pin (D) as in conventional electrospray system, Accumulated liquid destabilises spraying process in (E) because droplet is ejected from the pin, interfering with the mist. (**F**) Unwanted behaviour when voltage is high and sparkling between electrodes happen. This phenomenon is more prone to happen to sharper pins as they require lower voltage to generate corona discharge.

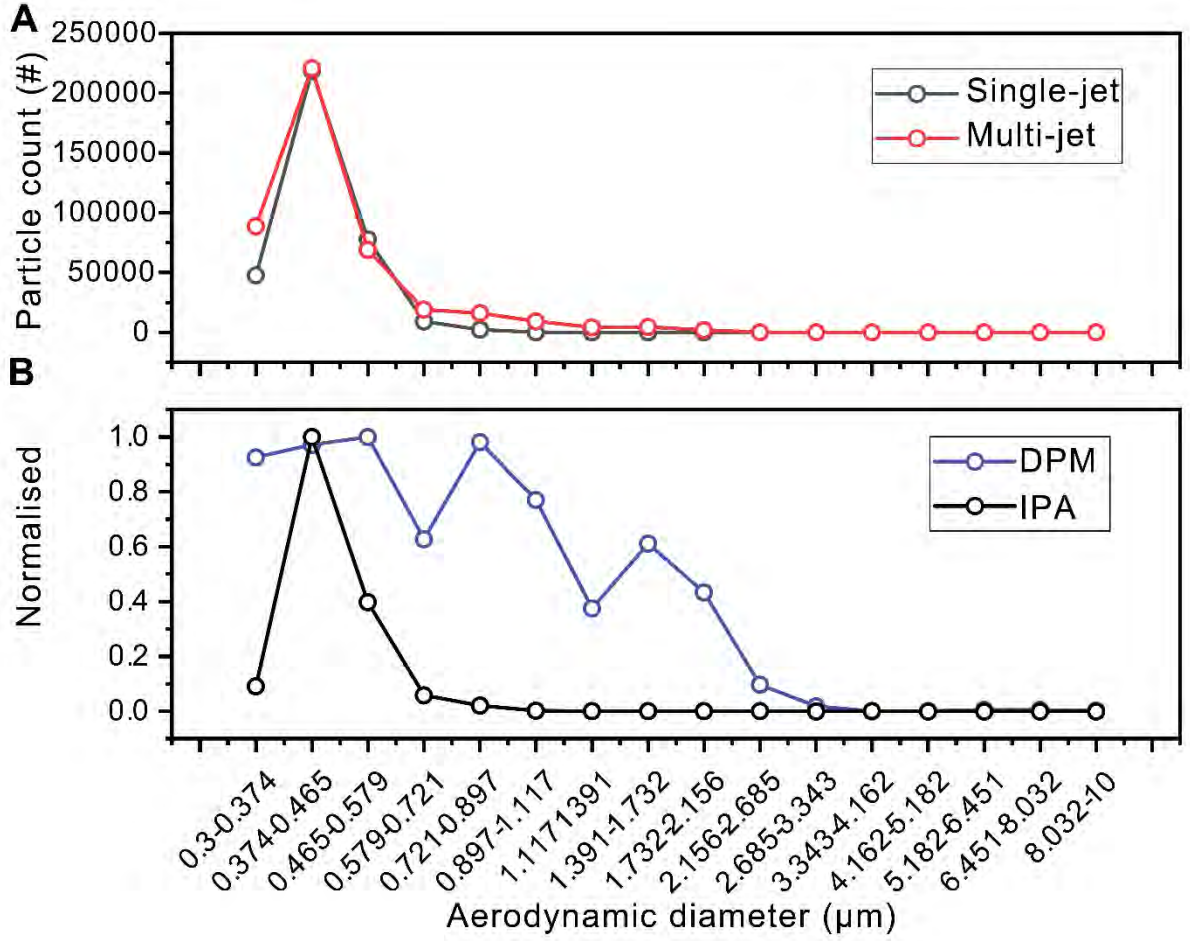

Fig S5: Size distribution in different modes and solutions. (**A**) Size distribution of IPA in different spraying mode, (**B**) Size distribution of particles generated from DPM and IPA.

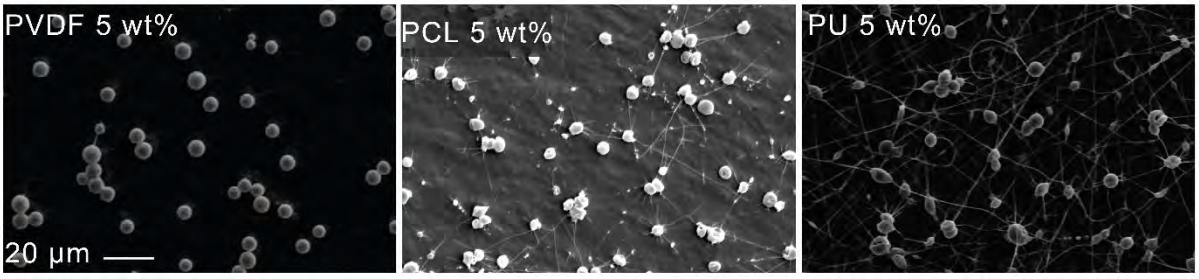

Fig S6. Morphologies of various polymers at 5 wt% concentration at 10 cm distance. Constant flow rate of 1.5 ml/hr with voltage varies between 4.3 to 4.8 kV.

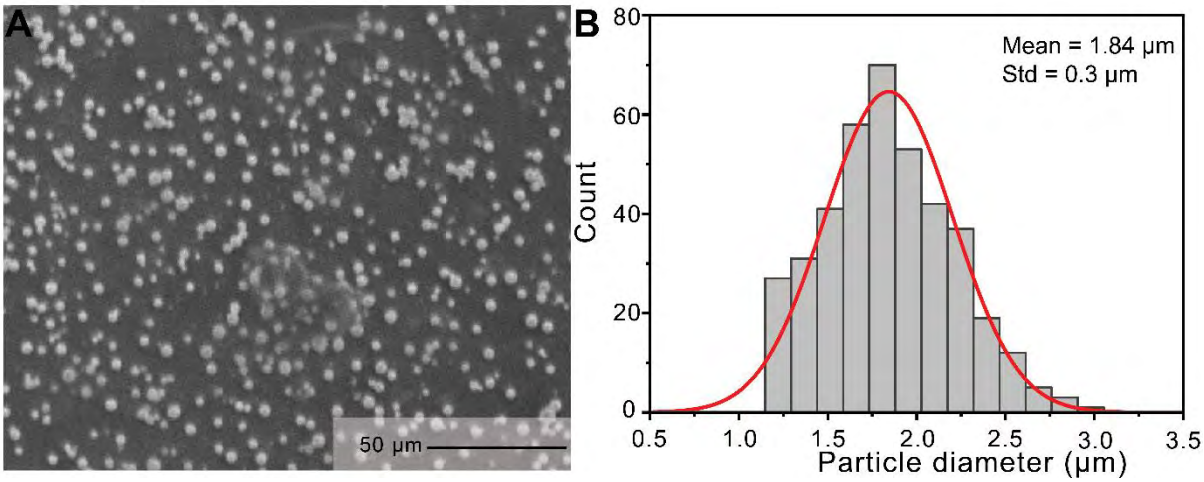

Fig S7. (**A**) PVDF 5wt% at 10 cm with 0.5 ml/hr flow rate on fixed cells. (**B**) Size distribution of particles. Number of sample: 400; average diameter: 1.84 µm; standard deviation: 0.3 µm.

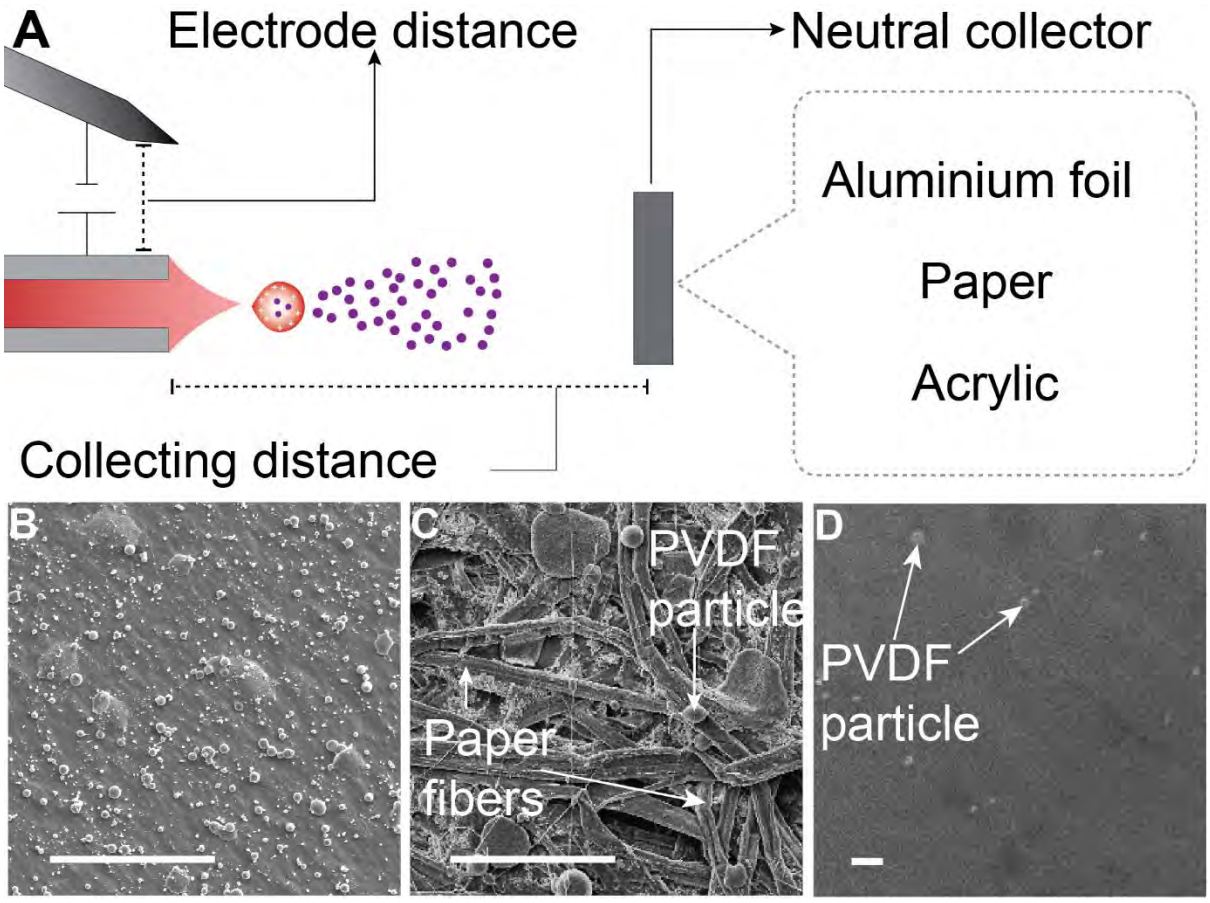

Fig S8. Deposition of PVDF particles onto free collector made from various material. (**A**) Schematic setup. (**B**) PVDF particles collected on aluminium foil. Aluminium foil is a suitable collector in conventional electrospray due to its conductivity and it is connected to one polarity of the system. In our system, free collector is an independent component that is not connected to electrical source. (**C**) Deposited PVDF particles on paper substrate. Paper is selected as collector due to its low electrical conductivity. SEM image show that PVDF particles are well deposited and adhered to the paper's

surface. (**D**) Deposited PVDF on an acrylic substrate. The surface of acrylic sheet is as smooth as aluminium foil's surface. Scale bar is 100 µm for all images.

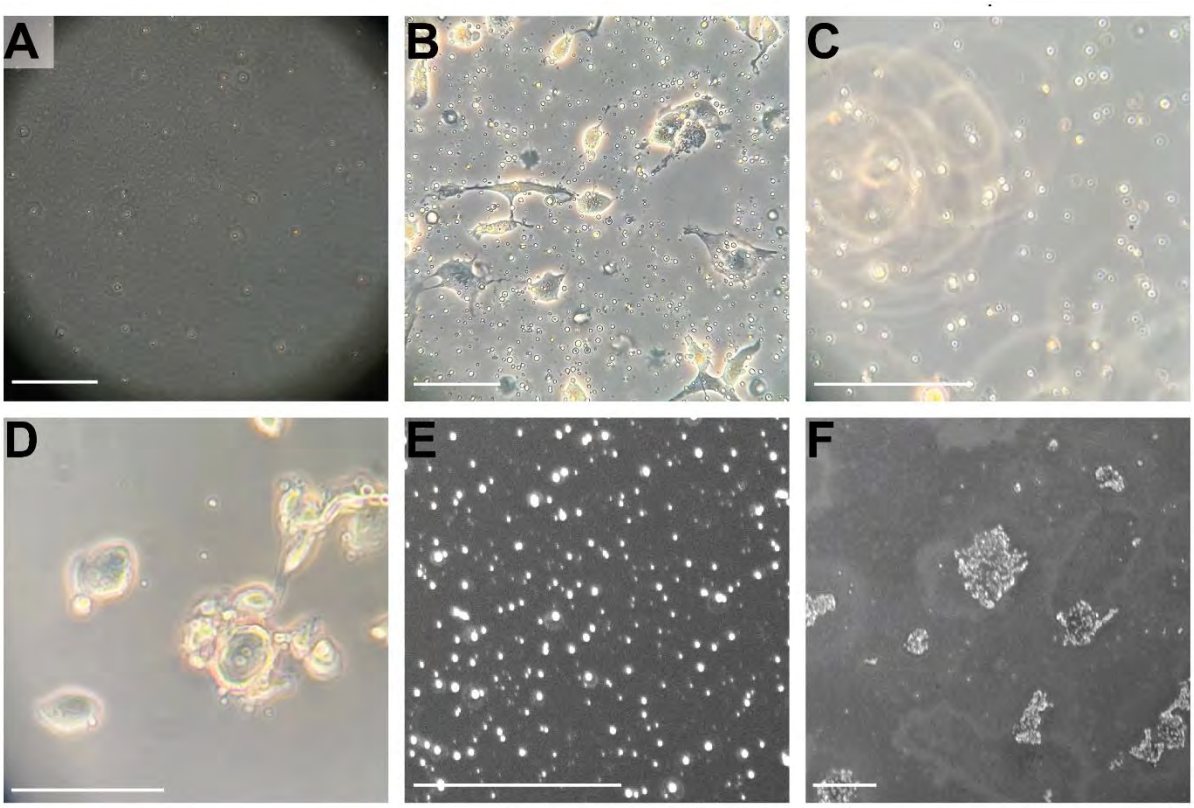

Fig S9. Deposited PVDF particles on Petri dishes of cells under conventional microscope and SEM. (**A**) PVDF particles deposited to Petri dish. (**B**) PVDF particles on cells after spraying experiment. Medium is removed prior to spraying experiment to ensure the contact and adhesion between cells and particles. (**C-D**) Images after culture medium is added back to Petri dishes to grow particles adhered cells after experiment. Images are taken at different focal planes, revealing a number of particles float freely in medium while others attach well to cells. Particles are floating in the culture medium as the focal plane shows no cells, as seen in (C). When focal plane changes, cells with particles in (D) displays the bond of particles and cells. This shows that particles are still attached to the cell after medium is added. (**E-F**) Deposited PVDF particles under SEM with and without cells. PVDF particles are deposited to an empty Petri dish for observation as seen in (E) as a reference for particles without cells. For the observation of particles with cells under SEM, fixation of cells prior to observation is conducted. After experiments, PFA is added to the Petri dish then removed after 10s to fix the cells. The action of adding and removing PFA liquid removes majority of floating particles (particles that are not adhered to cells) but well bonded cells (cells which particles adhere to) can be seen in (F) and manuscript. Scale bar is 100 µm for all images.

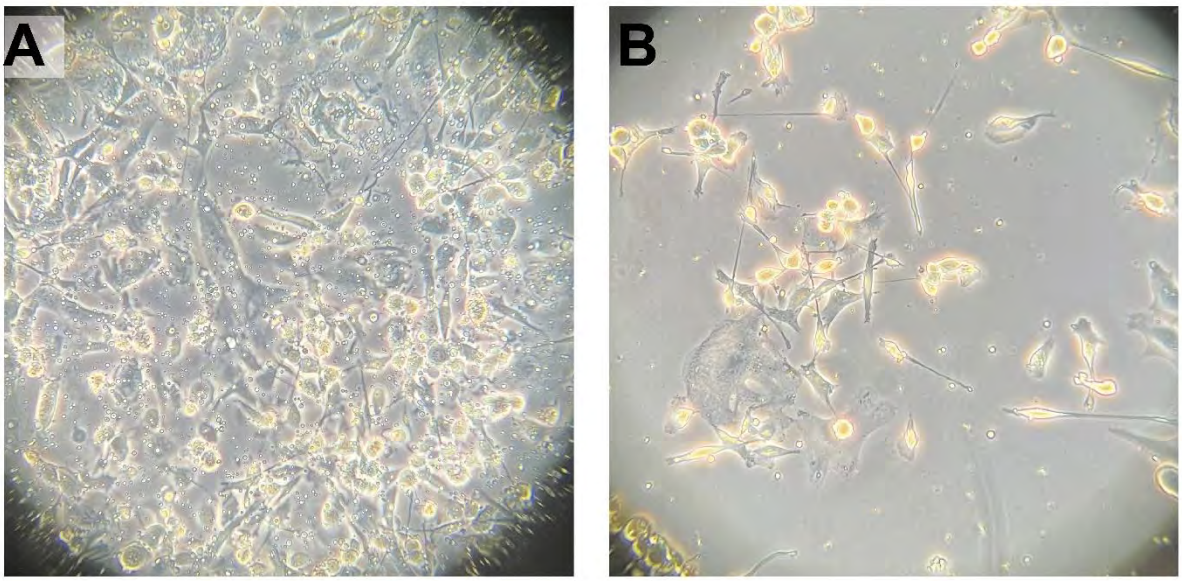

Fig S10. Deposited PVDF particles on Petri dishes of cells after spraying at various distances. (**A**) Cells are covered by particles in collecting distances of 5 cm and (**B**) of 10 cm after the same spraying period 30s.

References:

[1] C. Saputra, A. I. Kamil, M. M. Munir, A. Waris, Novitrian, *Aerosol Sci. Technol.* **2021**, *56*, 117.

[2] W. S. Mustika, D. A. Hapidin, C. Saputra, M. M. Munir, *Adv. Powder Technol.* **2021**, *32*, 166.

[3] L. M. M. Costa, R. E. S. Bretas, R. Gregorio, *Mater. Sci. Appl.* **2010**, *01*, 247.

[4] M. Wang, Q. Zhao, *Encycl. Biomed. Eng.* **2019**, *1–3*, 330.

[5] W. E. Teo, S. Ramakrishna, *Nanotechnology* **2006**, *17*, DOI 10.1088/0957-4484/17/14/R01.

[6] R. T. Steipel, M. D. Gallovic, C. J. Batty, E. M. Bachelder, K. M. Ainslie, *Mater. Sci. Eng. C* **2019**, *105*, 110070.

[7] S. K. Boda, X. Li, J. Xie, *J. Aerosol Sci.* **2018**, *125*, 164.

[8] S. Kavadiya, P. Biswas, *J. Aerosol Sci.* **2018**, *125*, 182.

[9] M. Ali, *Pulmonary Drug Delivery*, Vitthal S. Kulkarni, **2010**.

[10] Z. Farzal, S. Basu, A. Burke, O. O. Fasanmade, E. M. Lopez, W. D. Bennett, C. S. Ebert, A. M. Zanation, B. A. Senior, J. S. Kimbell, *Int. Forum Allergy Rhinol.* **2019**, *9*, 746.

[11] J. D. Suman, B. L. Laube, R. Dalby, *Pharm. Res.* **1999**, *16*, 1648.

[12] D. O. Frank, J. S. Kimbell, S. Pawar, J. S. Rhee, *Otolaryngol. Head. Neck Surg.* **2012**, *146*, 313.

[13] R. N. Dalby, S. L. Tiano, A. J. Hickey, **n.d.**

[14] D. N. Nguyen, C. Clasen, G. Van den Mooter, *J. Pharm. Sci.* **2016**, *105*, 2601.

[15] Q. T. Zhou, P. Tang, S. S. Y. Leung, J. G. Y. Chan, H. K. Chan, *Adv. Drug Deliv. Rev.* **2014**, *75*, 3.

[16] A. R. Rezk, J. K. Tan, L. Y. Yeo, *Adv. Mater.* **2016**, *28*, 1970.

[17] V. N. Morozov, *J. Aerosol Sci.* **2011**, *42*, 341.

[18] A. Carrasco-Munoz, E. Barbero-Colmenar, E. Bodnár, J. Grifoll, J. Rosell-Llompart, *J. Aerosol Sci.* **2022**, *160*, DOI 10.1016/j.jaerosci.2021.105909.

[19] L. Y. Yeo, Z. Gagnon, H. C. Chang, *Biomaterials* **2005**, *26*, 6122.

[20] L. Y. Yeo, D. Lastochkin, S. C. Wang, H. C. Chang, *Phys. Rev. Lett.* **2004**, *92*, 2.

[21] L. Zhu, M. Li, X. Liu, Y. Jin, *ACS Omega* **2017**, *2*, 2273.

[22] Z. Mai, J. Chen, T. He, Y. Hu, X. Dong, H. Zhang, W. Huang, F. Ko, W. Zhou, *RSC Adv.* **2017**, *7*, 1724.

[23] D. M. Correia, R. Gonçalves, C. Ribeiro, V. Sencadas, G. Botelho, J. L. G. Ribelles, S. Lanceros-Méndez, *RSC Adv.* **2014**, *4*, 33013.